

2013

Automated sinkhole extraction and morphological analysis in northeast Iowa using high-resolution LiDAR data

Jonathon Launspach
University of Northern Iowa

Let us know how access to this document benefits you

Copyright ©2013 Jonathon Launspach

Follow this and additional works at: <https://scholarworks.uni.edu/etd>



Part of the [Geography Commons](#)

Recommended Citation

Launspach, Jonathon, "Automated sinkhole extraction and morphological analysis in northeast Iowa using high-resolution LiDAR data" (2013). *Dissertations and Theses @ UNI*. 33.

<https://scholarworks.uni.edu/etd/33>

This Open Access Thesis is brought to you for free and open access by the Student Work at UNI ScholarWorks. It has been accepted for inclusion in Dissertations and Theses @ UNI by an authorized administrator of UNI ScholarWorks. For more information, please contact scholarworks@uni.edu.

Offensive Materials Statement: Materials located in UNI ScholarWorks come from a broad range of sources and time periods. Some of these materials may contain offensive stereotypes, ideas, visuals, or language.

AUTOMATED SINKHOLE EXTRACTION AND MORPHOLOGICAL ANALYSIS
IN NORTHEAST IOWA USING HIGH-RESOLUTION LIDAR DATA

An Abstract of Thesis
Submitted
in Partial Fulfillment
of the Requirements for the Degree
Master of Arts

Jonathon Launspach
University of Northern Iowa
August 2013

ABSTRACT

Accurate and detailed mapping of sinkholes is necessary to ensure sinkhole monitoring and management. Historically, sinkholes were found and digitized manually by a visual examination of aerial photos or through field surveying. This paper develops a new, multicriteria LiDAR-based sinkhole extraction method and automated processes to detect sinkholes and their boundaries. This technique of extraction is unique as it identifies sinkhole boundaries automatically using remotely sensed data, compared to traditional methods of manually tracing the perimeter. A sinkhole detection module was developed within a GIS environment to determine location and boundaries of the sinkholes. Several small study areas were selected to test different extraction methods. Three tested methods included the fill, slope and object-oriented methods. A combination of the fill and slope methods demonstrated the most reliable extraction results. A geoprocessing model and Python scripting was then implemented to automate the procedure. This automated sinkhole extraction method was applied to the entire study area in northeast Iowa. The primary data for the study were one meter Light Detection and Ranging (LiDAR) dataset. Aerial photos, GPS, and existing sinkhole data were used for method calibration and accuracy assessment. The second part of the study focused on the sinkhole quantitative characteristics derived from the LiDAR based sinkhole map. The characteristics include perimeter, area, shape, maximum depth, lineation, and orientation. Statistical analysis was then performed in order to determine geometric patterns, morphological and generic groupings, and possible correlations with geomorphic and environmental parameters.

AUTOMATED SINKHOLE EXTRACTION AND MORPHOLOGICAL ANALYSIS
IN NORTHEAST IOWA USING HIGH-RESOLUTION LIDAR DATA

A Thesis
Submitted
in Partial Fulfillment
of the Requirements for the Degree
Master of Arts

Jonathon Launspach
University of Northern Iowa
August 2013

This Study by: Jonathon Launspach

Entitled: AUTOMATED SINKHOLE EXTRACTION AND MORPHOLOGICAL ANALYSIS IN NORTHEAST IOWA USING HIGH-RESOLUTION LIDAR DATA

has been approved as meeting the thesis requirement for the

Degree of Masters of Arts

_____	_____
Date	Dr. Patrick Pease, Chair, Thesis Committee
_____	_____
Date	Dr. Andrey Petrov, Thesis Committee Member
_____	_____
Date	Dr. David May, Thesis Committee Member
_____	_____
Date	Dr. Bingqing Liang, Thesis Committee Member
_____	_____
Date	Dr. Michael J. Licari, Dean, Graduate College

TABLE OF CONTENTS

	PAGE
LIST OF TABLES	vi
LIST OF FIGURES	vii
CHAPTER 1. INTRODUCTION	1
Research Goals and Objectives.....	3
CHAPTER 2. LITERATURE REVIEW	4
Introduction.....	4
Karst Plains	5
Sinkholes (Dolines) and Development	7
Sinkhole Examination Methodology	8
State of Knowledge on Sinkhole Distribution	11
LiDAR and Digital Elevation Models	14
Sinkholes and LiDAR	16
Environmental	18
Sinkholes in Iowa	18
CHAPTER 3. STUDY AREA AND METHODOLOGY	21
Study Area	21
Geological Characteristics of the Study Area	25
Data	28
LiDAR.	28
Geologic	28

Physical and Infrastructure Variables	28
Field Data Collection	30
Data Processing	33
Sinkhole Identification Methodology	35
Automated Identification Model for Sinkholes (AIMSINK)	35
Submodel 1: Slope Extraction	35
Submodel 2: Filling Closed Depressions	36
Submodel 3: Combining Fill and Slope to Identify Sinkhole Boundaries	36
Submodel 4: Calculating Sinkholes Area and Axes	37
Submodel 5: Eliminating of Non-Sinkhole Features	38
Outside of Model: Additional Elimination of Non-Sinkhole Features	39
Submodel 6: Extracting DEM Data for Identified Sinkholes	40
Accuracy Assessment Methods	43
Preparing Features for Geomorphological Analysis	43
Location and Geomorphologic Analysis Methodology	44
CHAPTER 4. RESULTS AND DISCUSSION	47
AIMSINK Results and Accuracy Assessment	47
Statistical Analysis	50
Spatial Analysis	54
Sinkhole Clustering	54
Spatial Patterns of Sinkhole Characteristics	55
Alternative Methods of Sinkhole Identification Tested in This Study	61

Object-Oriented Method	61
Curvature Method	63
CHAPTER 5. CONCLUSION AND LIMITATIONS	66
Conclusions	66
The AIMSINK Model	66
Sinkhole Characteristics and Distribution	67
Limitations	69
Methodological Limitations	69
Data Errors	70
Future Work	71
REFERENCES	72
APPENDIX: ALMI AND HOTSPOT MAPS	78

LIST OF TABLES

TABLE	PAGE
1 List of data used and their sources	30
2 Accuracy assessment of AIMSINK in two study areas based three methods	49
3 Correlation table of sinkhole variables	52
4 PCA of sinkhole variables.....	53
5 K Means clustering of sinkhole variables broken into five categories.....	54
6 Global Moran's I of all variables showing clustering of all values	56
7 The graph displays the sinkhole variable groupings among each region	59

LIST OF FIGURES

FIGURE	PAGE
1 General locations of karst around the world	5
2 Illustrates the process of LiDAR data collection based on aerial collection	15
3 Distribution of sinkholes throughout Iowa based on the DNR; the numbers displayed illustrate the amount of sinkholes within that data set	23
4 A hillshade image of study area 1 allowing visual identification of sinkholes	24
5 A hillshade image of study area 2 of the dense sinkhole landscape	24
6 Illustration of the stratigraphic column within Northeast Iowa	26
7 A bedrock geology map of Northeast Iowa; data source IDNR	27
8 Study area 2 showing the general topography of the region	31
9 A sinkhole in study area 2, photographed during GPS boundary measurement	32
10 An Uvala formation in study area 2	32
11 A major sinkhole in study area 1 and surrounding farm field	33
12 The Completed AIMSINK model	41
13 Left side of model	42
14 Right side of model	42
15 A Map of 47,445 sinkholes identified by the AIMSINK model.	48
16 The image illustrates the accuracy of three sinkholes utilizing three different techniques. Yellow represents the boundary that was collected using GPS. Blue represents the boundary of the AIMSINK model and Red represents the boundary of the heads up digitizing the Iowa DNR produced based on the LiDAR data	49
17 Ripley's K function of entire study area	55
18 Composite clustering groups from Moran's I and LISA models. See Table 7 for clustering patterns of end groups	60

19 Curvature image that was utilized for object-oriented classification62

20 Results from object-oriented classification.....62

21 Curvature description of different combinations: The top three shapes represent the difference in values that can be acquired from profile curvature. The bottom three represent the difference in values that can be acquired from profile view. A combination of these can create a curvature output.....64

22 Study Area 2 curvature profile map.....64

23 Study Area 2 curvature profile classification attempt map.....65

CHAPTER 1

INTRODUCTION

Karst Plains are large flat surfaces which develop by erosion and corrosion; they have been studied by geomorphologists for years and are considered one of the primary fields in karst research. Karst plains are predominantly studied in Europe and parts of the United States including Indiana, Kentucky, Tennessee, and Florida (Harmon, Wicks, Ford, & White, 2006). Sinkholes are a common feature found within Karst plains and mainly occur in carbonate rock. Carbonate rock is soluble in water which over time allows these sinkholes to develop. In an effort to better understand sinkhole development, studies have examined morphometric features such as orientation, area, and volume to identify any spatial correlation among them (Galve et al., 2009, October 15; Palmquist, 1977; Williams, 1971). Other studies have analyzed sinkhole distribution and morphologies in an effort to model their development or to better manage them as a natural hazard (Gao, Alexander, & Barnes, 2005; Zhou, Beck, & Adams, 2003). A majority of the studies have focused on a few areas with well-developed karst landscapes. Smaller karst landscapes, such as Iowa, have been studied less due to the relatively limited spatial occurrence of sinkholes (Gao, Alexander, & Barnes, 2005). Northeast Iowa and Southwest Minnesota fall within these smaller subsets of karst areas. However, even though this area is relatively small compared to others, it still has a diverse variety of sinkholes (Palmquist, 1977; Prior, 1991). The study of their characterization and development may provide a valuable insight into sinkhole morphology patterns and formation processes.

The goal of this study is to develop a comprehensive tool to locate and accurately characterize sinkholes over a large region. This will drastically improve the efficiency of sinkhole identification process compared to traditional (manual) methods. Such a comprehensive and automated methodology has not been offered before and should provide a better understanding of the distribution, morphology, and typology of sinkholes specifically within the Northeast Iowa Karst region. Enhancing knowledge about karst morphology and genesis is necessary to assist in agricultural activities, as well as to aid in the mitigation and infrastructure development processes (Huber, 1989). Farming and groundwater contamination can be accelerated within this area, due to the connection between surficial water and ground water through the karst landscape and specifically sinkholes (Gao, Alexander, & Tipping, 2005; Huber, 1989; Prior, 1991).

Newer techniques, such as Light Detection and Ranging (LiDAR), are starting to be used for sinkhole identification as they provide high resolution continuous data over larger areas, giving it a great advantage over traditional techniques. The only recent use in Iowa was by the Iowa Department of Natural Resources (DNR), although DNR performed manual identification of sinkholes in a limited area. In addition, very little spatial and statistical analysis has been performed on the sinkholes found in Iowa the only notable study was completed in 1977 (Palmquist, 1977) as well as sites studied by the DNR on small isolated areas (Groves, Walters, Day, Hubsher, & SEPM Fall Field Conference, 2008; Wolter, McKay, Liu, Bounk, & Libra, 2011). This study aims to contribute to closing this significant knowledge gap.

Research Goals and Objectives

The goal of this study is to develop an automated process and use LiDAR-based methodologies for detection of karst features over a larger area and to improve our understanding of sinkhole distribution and typology in Northeast Iowa.

This research intends to address the following questions:

1. What is the best methodology to take advantage of LiDAR data and create an automated method for sinkhole location and morphology?
2. Can LiDAR-derived morphologic characteristics be used to classify sinkholes based on size, geometry, and geologic/geomorphic settings?
3. Are there discernible spatial patterns in sinkhole distribution, such as clustering, striations, or nucleation, and are there correlations between the size and geometric characteristics of sinkholes and the local setting, such as slope, lithology, or elevation?

The practical contribution of this study is the development of a tool for automated identification of sinkholes that can become a key element in an emerging comprehensive system of sinkhole monitoring and management on the other hand, this will help contribute to the field of karst geomorphology, as it gives a unique insight in to a wide range of geomoprological characteristics over a much larger area of sinkhole development compared to previous studies examining smaller regions.

CHAPTER 2

LITERATURE REVIEW

Introduction

Karst regions are defined by the presence of soluble rock, primarily limestone, and characterized by specific soluble features (Jennings, 1985). Numerous studies have examined karst geomorphology over the years in various locations. One of the original locations of karst research was Slovenia. The term was first used there meaning “stony, barren ground” (Ford & Williams, 2007). One of the first researchers to provide the base for karst studies was Jovan Cvijic (Ford & Williams, 1989). He produced a comprehensive study of karst, and today he is considered one of the founding fathers of karst research (Harmon et al., 2006).

Karst landscapes are common throughout the world; they comprise approximately 20% of the Earth’s surficial rock; and 15% of the United States is made up of soluble aquifers (Herak & Stringfield, 1972; Figure 1). In addition, 25% of the world’s population obtains their water from carbonate karst rock (Ford & Williams, 1989). The most suitable type of rock to develop carbonate karst characteristics is a rock that is dense, massive, and coarsely-fractured. Rocks that are highly porous, around 30-50%, are usually less likely to develop karst characteristics within them (Ford & Williams, 2007). Most karst areas are comprised of rock from two groups: evaporite and carbonate rocks. The evaporite rocks include halite, calcite, anhydrite, aragonite, and gypsum. The most

predominate karst development is carbonate rock primarily consisting of limestone and dolomite (Ford & Williams, 2007).

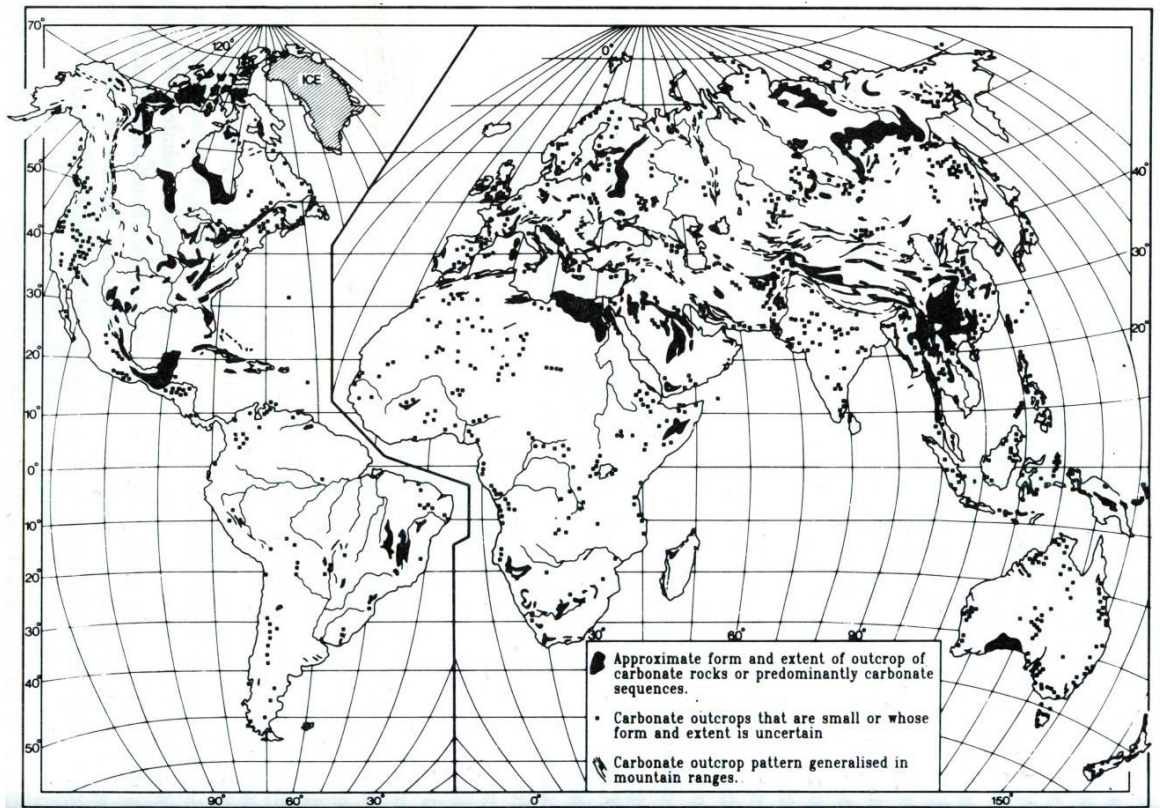


Figure 1: General locations of karst around the world.

(Ford & Williams, 1989, p.4)

Karst Plains

Karst Plains are large flat surfaces which develop by erosion and corrosion. The plains can be rather large; some tens of square kilometers in size (White, 1988). When soluble bedrock becomes exposed, ground water pirates the surface flow ending the development of surface valleys; the drainage then becomes internal, causing surface

stripping laterally due to the lack of entrainment. Overtime this procedure produces a karst plain. The key factors that determine the development are geologic structure, relief, hydrology, climate, lithology, vegetation, and time (Jennings, 1985). These surfaces are typically composed of sinkholes, along with many other karst features, such as blind valleys, uvulas, and sinking streams. Karst plains are not spatially restricted by faults or other geologic factors, whereas other karst features may be (White, 1988). The main karst plains in the U.S. are the Valley and Ridge province of the Appalachian Mountains, Edwards Plateau, south-central Indiana, west-central Kentucky, Central Florida, and east-central Missouri (Ritter, 1978).

Karst (sinkhole) plains are the most widely represented of karst landscape types (White, 1988). These sinkholes are usually distributed in variable patterns and they come in a variety of shapes and sizes; however, in some instances they are delineated by line patterns (Sweeting, 1981). The well-known areas in the United States are the Mitchell Plain of Southern Indiana, Pennyroyal Plateau in Kentucky, and the Highland Rim of central Tennessee (Jennings, 1985; Pease, Gomez, & Schmidt, 1994; Sweeting, 1973; White, 1988). Sinkhole distributions have been studied in less well-known areas. For example Northeast Iowa and Southeast Minnesota where the sinkholes are less developed as compared to other well-studied regions (Gao, & Alexander, 2008; Groves et al., 2008; Prior, Grant, & Geological Society of Iowa, 1975).

Sinkholes (Dolines) and Development

Dolines or sinkholes are defined as closed depressions found in karst regions (Jennings, 1985). Sinkhole depressions can range in size from half a meter in depth to several hundred meters. A sinkhole diameter can vary from a few meters to several hundred meters in size (Jennings, 1985; White, 1988). Sinkhole characteristics are typically dependent on the age of the karst landscapes. Over time small sinkholes tend to merge together to form a larger sinkhole known as a uvula (Summerfield, 1997).

Sinkholes can develop in numerous ways. A majority of sinkholes are formed by dissolution of bedrock by percolated surface water. Rainwater becomes acidic by dissolving CO₂ as it moves through the soil. The resulting carbonic acid disassociates carbonate molecules in the process:



Collapsing, piping, and subsidence can contribute in creating sinkhole features (Jennings, 1985). The dissolution of the rock through a chemical reaction allows for the rock to dissolve and be removed in solution. Over time, conduit forms through dissolution of limestone allowing surface water to connect to the underlying ground water or caves. Few studies have examined the correlation between sinkholes and cave development (Shofner, Mills & Duke, 2001).

The amount of water being added to the depression or point of recharge plays a key role in the time it takes for the sinkholes to develop, in addition to the vegetation and

soil thickness (Summerfield, 1997; Wilson & Beck, 1992). The thickness and amount of vegetation can slow the chemical weathering and erosion processes on the rocks below (Summerfield, 1997). However, more vegetation can increase the soil solution weathering process due to the rise in carbon dioxide it consumes (Ritter, 1978). Climate can also be an important factor in sinkhole development. An area that is normally warmer and wetter is capable of developing sinkholes at a much higher rate. This is due to the chemical weathering process allowing the rock to break down at a greater rate. This can be seen when comparing locations in the United States to those in Jamaica or New Guinea (Harmon et al., 2006).

Sinkhole Examination Methodology

Studies in the past have used manual methods to analyze sinkholes. A pioneer study on this subject focused on the morphometric analysis of polygonal karst in New Guinea (Williams, 1971). This study examined sinkhole landscapes and their correlation to networking karst. It showed that well-defined sinkhole plains tend to form connected pentagonal structures. The study took into account three types of polygonal karst, which consisted of pinnacle, conic, and linear. It determined area, length, width, ratio, symmetry, and orientation, as well as calculated nearest neighbor distribution to try to understand how this sinkhole plain had developed.

Another similar analysis was performed by Sweeting (1973). This paper analyzed the correlations between percent area drained, structure orientation, and alignment/elongation using a logarithmic scale. It demonstrated that there was also a correlation

between the surface karst and the drainage patterns (Sweeting, 1973). These spatial analysis patterns were some of the first well-documented examples. A more recent analysis in Northeast Spain examined evaporite collapse sinkholes. This was done using GPS, aerial photos, and field observations, which were all used to identify the increase in sinkhole activity. These studies took into consideration the following: mean area, total area, maximum area, maximum length, mean length or diameter, maximum depth, mean depth, and total volume (Guerrero, Gutierrez, Bonachea, & Lucha, 2008; Gutierrez, Cooper & Johnson, 2008). Several studies have combined the analysis of morphologies and spatial distribution. In particular, a study in Florida utilized GIS and topographic maps to digitize 25,000 sinkholes. The study then identified depth, major axes, circularity, length/width, mean diameter, width, length, perimeter, and depression area and analyzed correlations and spatial patterns (Denizman, 2003). Their finding identified that GIS is capable of removing human error and provides an efficient way of analyzing sinkholes and their characteristics. The limitations to the study consisted of resolution with five feet contour lines, and the possible human error in manually digitizing.

More advanced procedures were utilized in a study analyzing spatial distribution and pattern of sinkholes in Maryland along I-70 based on the Gibbsian Point process and the Strauss Model (Zhou et al., 2003). It was found there was a correlation between distance and orientation of the examined sinkholes. The Strauss Modeling was then performed with seven key factors including topography, proximity to topographic depressions, interpreted rock formation, soil type, geophysical anomalies, proximity to

geologic structures, and thickness of overburden. This process was also used to more accurately predict where future sinkholes may develop (Zhou et al., 2003).

Other models have been developed specifically looking at nearest neighbor relationships among sinkholes. For example, Galve et al. (2009, January 1) evaluated and compared methods of estimating sinkhole susceptibility by mapping evaporite karst in the Ebro Valley. Several different methods were included: sinkhole density, probabilistic analysis, heuristic scoring, and, most importantly, the nearest-neighbor distance. The nearest neighbor analysis was found to be the most accurate and reliable, while other models varied significantly. The research also pointed out that in order to make the models more accurate, the appropriate and most relevant information must be obtained (Galve et al., 2009, October 15). A similar model was developed to identify the key variables that affect sinkhole development in the Northeast portion of Spain (Lamelas, Marinoni, Hoppe, & Riva, 2008). The results were then processed using logistical regressions to determine these key variables. The model concluded that sediment thickness is a primary variable and several environmental factors play a significant role in developing sinkholes (Lamelas et al., 2008).

These models allow one to determine the factors that are most applicable to sinkhole development. Using newer technology, several recent studies were able to produce sinkhole density models, such as Gao, Alexander, and Barnes (2005) study of sinkhole distribution. This paper tested some of the traditional techniques used in sinkhole analysis, referring to the nearest neighbor analysis, as well as distinctive sizes of

sinkholes plains and their clusters. Sinkhole density, orientation, and distribution were also taken into account. They created what they call a Karst Feature Database (KFD) that allows incorporating multiple layers to eventually analyze what factors are the most influential to sinkhole risk and development (Gao, Alexander, & Barnes, 2005).

In summary, most existing studies focused on analyzing the overall distributions and correlation among sinkhole characteristics, as well as implementing other criteria into the analysis to better understand sinkhole distribution. In particular, several studies examined distribution using nearest neighbor methods, which also included the analysis of different morphological characteristics, such as shape, size, and orientation (Williams, 1971; Jennings, 1985). Other studies developed models to try to understand the distribution and predict formation of future sinkholes using various factors (Gao, Alexander, & Barnes, 2005; Galve et al., 2009, January 1; Zhou et al., 2003). Many of these models have incorporated the key factors to identify sinkholes and their distribution; however they haven't taken into consideration the use of LiDAR in a large study area. LiDAR is much higher resolution than many of the previous studies have used and provide much better results.

State of Knowledge on Sinkhole Distribution

Sinkhole Distribution is key to understanding the development and what factors may drive them, and how they could be affected or affecting urban areas. Sinkholes develop based on geologic structural attributes, the differences between the shape and size are a direct result of the terrain based where they are found. Geological and climatic

characteristics allow them to grow from small individual sinkholes to compound sinkholes or uvalas (Ford & Williams, 2007). The key to development of sinkholes is the draw down in ground water levels produced by an initial sinkhole that introduces a hydraulic gradient that removes soil cover and removes sediments from joints (White, 1988).

Geomorphologists have determined sinkhole characteristics by examining the distribution of sinkholes in various regions of the world (Denizman, 2003; Hyland, Kennedy, Younos, & Parson, 2005; Galve et al., 2009 January 1; Gao, Alexander, & Tipping, 2005; Whitman, Gubbels & Powell, 1999; Williams, 1971; Zhou et al., 2003). The main types of analysis include the examination of growth patterns, change over time, and change in patterns in space. Sinkhole volume is very similar to a cone shape; therefore the depth typically increases with a growing surface area. Another example, cockpit karst can form due to a thick layer of carbonate rock forming small valleys and even creating small river networks within. In this instance, the depth and area have no correlation between them (Ford & Williams, 2007).

Sinkholes have been identified as having a variety of distribution patterns and morphological characteristics throughout the world. An early analysis of karst morphologies was done by Williams (1971) in New Guinea. This research demonstrated a developed network of sinkholes or pitted landscape. This landscape was identified as a uniform, cellular network of polygonal karst. Small identical features grew over time forming these features as they were subject to the development only within the karst

region. If the sinkholes grew large enough, they would merge adjacent boundaries and form uvulas, however, still holding the structural shape (Williams, 1971).

A study in Virginia determined the relationship between four factors as keys to sinkhole development. These factors consisted of the depth of soil to bedrock, proximity to geologic faults, and proximity to surface streams. The key findings were that sinkholes are sparse near streams, they are primarily found in pure carbonate rock of Ordovician age, and they are more prone to occur near fault lines (Hyland et al., 2005). Another study in Maryland showed similar characteristics with geology playing a key role in the distribution, with irregular bedrock surfaces, easily erodible soil, and well-developed joint systems within the rock. The distribution, however, was irregular, but with clustering patterns mostly occurring within a 30- meter radius of each other. Intensive land use caused more of these to develop within those areas (Zhou et al., 2003).

Southeastern United States has rather unique karst, especially in Florida, where several reports illustrated a correlation between water table and clustering. This illustrates the importance of hydrostatic loads in sinkhole hazards within the region (Whitman et al., 1999). Others point out recharge areas are significant on specific surfaces, in this case elevated sandy ridges. Most sinkholes develop during certain times of the year around April and May as this point is the normal low for ground water (Wilson & Beck, 1992). Some areas, however, show little signs of spatial patterns with variation in small regions (Denizman, 2003). Analysis of sinkholes in Minnesota has demonstrated slightly different results (Gao, Alexander, & Tipping, 2005). The study showed sinkholes in that region tend to form in highly concentrated zones. The clustering changes, however,

depending on the scale of 2-100 km². The study also demonstrated sinkholes tended to form in similar geologic and geomorphic settings. In addition, the hydraulic gradient impacted newly forming sinkholes. It was also evident sinkholes may follow linear terrain trends. Evidence illustrated sinkholes developed differently between the Cedar Valley and Galena/Spillville Karst and Prairie du Chien Karst with more clustering in the Cedar Valley and Galena/Spillville Karst. Certain counties within the study area exhibited clustering parameters; however, others did not. (Gao, Alexander, & Tipping, 2005).

Other regions of the world, for example Spain, illustrate similar findings as pertains to the distribution of sinkholes. Elevation among different terrace levels played a key role in the sinkhole development and distribution (Lamelas et al., 2008). The second primary factor identified was irrigation practices and their impact on the water table gradient (Lamelas et al., 2008). Other regions of Spain have illustrated joint sets have been the major contributor to the development of the sinkholes (Galve et al., 2009, January 1).

LiDAR and Digital Elevation Models

LiDAR stands for Light Detection and Ranging and uses the same principles as other active remote sensing techniques. The LiDAR instrument directs short laser pulses to the Earth's surface (Vacher, Seale, Florea, & Brinkmann, 2008), and records the time it takes for the light to reflect back to the plane. The receiver records the time interval in fractions of a second calculating the distance based on the speed of light to determine

elevation. A GPS system acquires the position, and the location information is stored along with the LiDAR data in the file format, XYZ or LAS (Ritchie, 1995; Figure 2).

LiDAR has advanced the geomorphologic applications of remote sensing significantly. The elevation data produced in the past primarily ranged from ten to thirty meters resolution, which allowed only the analysis of large elevation structures. However, with the resolution of LiDAR on average being around one meter, it is possible to discern considerably smaller details, making it more effective, realistic, and accurate. The increases in accuracy and resolution have opened new opportunities to terrain analysis including the detection of sinkholes (Montane, 2001).

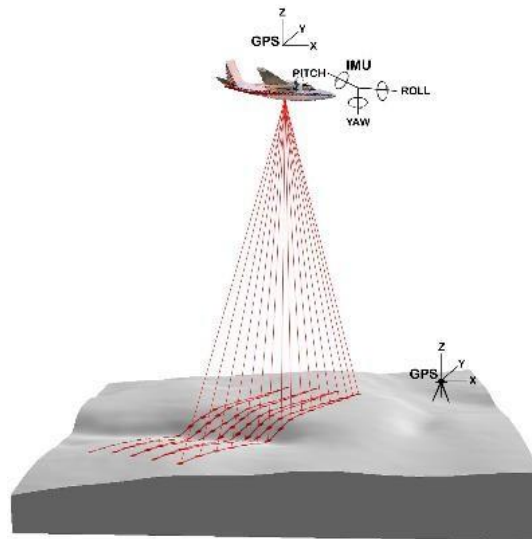


Figure 2: Illustrates the process of LiDAR data collection based on aerial collection.

(http://forsys.cfr.washington.edu/JFSP06/lidar_technology.htm, n.d.)

Digital Elevation Models (DEM) can be derived from several types of remote sensing data using a variety of techniques (Chang, 2008). The development of higher resolution DEMs has allowed scientists to study terrain features with much more detail than previously possible (Chang, 2008). Prior to LiDAR, the best DEMs were typically thirty-meter resolution. The coarse resolution had been a limiting factor in the use of DEMs for sinkhole studies because it made it difficult to distinguish smaller sinkholes.

Sinkholes and LiDAR

Recently, a number of researchers have analyzed sinkholes using LiDAR. Many of these studies have been methodological and focused on identifying the most suitable way to identify sinkholes using LiDAR. In conjunction with that process, they have been assessing the accuracy of LiDAR-based methods. For example, Seale, Florea, Vacher, and Brinkmann (2008) conducted a study in Pinellas County, Florida where sinkholes have already been recognized utilizing aerial photography and concluded with ground truthing methods. The objective of their study was to assess the accuracy of LiDAR compared to that of the original methods of aerial photography. They identified more sinkholes by LiDAR than by aerial photography; however closer examination of the results indicated their use of contours for sinkhole extraction resulted in a lower degree of accuracy and some depressions had outlets, identifying that these in fact were not sinkholes. The other problem they encountered was residential areas caused a problem as swimming pools and other round objects were detected as sinkholes. Therefore, it is

essential to assess the LiDAR data by ground truthing and aerial photography (Kruse, Grasmueck, Weiss, & Viggiano, 2006; Seale et al., 2008).

Other studies attempted to demonstrate whether LiDAR is able to distinguish the underlying geology as well. Several projects used ground-penetrating radar (GPR) to evaluate the accuracy of LiDAR. Montane (2001) examined a small area within Florida. Using LiDAR data to extract morphology, the accuracy was assessed using ground surveying. The GPR was then utilized to assess the underlying geology to determine if there was a correlation between surficial geology and bedrock geology. The results showed that the LiDAR was able to extrapolate some underlying features; however, it was not as accurate as it was hoped (Montane, 2001; Kruse et al., 2006).

Filin, Avni, Marco, and Baruch (2006) examined sinkhole distribution using LiDAR data in the Dead Sea region. They found, based off their model which utilized remote sensing techniques, that the sinkhole description is best featured by discontinuity of the first derivative of the DEM surface. The realization of this method gave a very clear appearance of sinkholes on the digital maps. This indicates the appropriateness of using LiDAR for detecting these geomorphic features. The study was also able to extract quantitative information about sinkholes, most importantly volumetric information, which gives an insight into soil erosion processes.

The analysis of the recent literature illustrates the LiDAR-based methodologies produce high quality results in respect to detecting and characterizing sinkholes. They also demonstrate the importance of further testing of LiDAR techniques as tools for

determining sinkhole distributions. In addition, the increasing volume of these types of studies will allow a better understanding of the dynamics of the whole karst system.

Environmental

Environmental studies have also been conducted on these sinkhole features due to their direct correlation with ground water and ground water quality (Hallberg & Hoyer, 1982; Huber, 1989; Parise, Waele, & Gutierrez, 2009). Several studies also investigated people's understanding and the possible implications that can occur if sinkholes are not dealt with properly (Huber, 1989). Mitigation plans have also been introduced to these karst sinkhole areas. They focus not only on the road and building structures, but also possible ways to eliminate probable contamination areas (Gutierrez et al., 2008; Zhou et al., 2003). Other studies have examined the impact people have made on karst (Podobnikar, Scho"ner, Jansa, & Pfeifer, 2008). Sinkholes can also have a significant impact on agricultural activities. Studies have examined the effects fertilizers and livestock have on sinkholes by determining infiltration rates or changing morphological characteristics (Boyer & Alloush, 2001). Given the important implications of karst in various domains of human activity, it is important to focus on analyzing karst in respect to environmental and hazardous consequences of sinkhole formation.

Sinkholes in Iowa

Although there has been a significant amount of research devoted to karst landforms, and sinkholes specifically, a greater diversity of field sites is needed to understand their development. Several studies have examined the distribution and factors

affecting sinkhole development in Iowa. Previous work has provided an insight into understanding karst geology in Iowa (Groves et al., 2008; Hallberg & Hoyer, 1982; Prior et al., 1975). Several studies were done in Iowa on the distribution of sinkholes. The analysis of Floyd County illustrated that solutional feature began forming during the Cretaceous time period (Palmquist, 1977; Prior et al., 1975). Since then they were covered by drift in some locations and have slowly been evolving into their present day shape. Morphometric factors identified with sinkholes in Iowa illustrated they were found to have intermitted streams ending in them. Uvulas are common with a majority of them developing vegetation such as shrubs and trees within them. The primary shape of sinkholes was funnel shaped with circular or oval outline, some illustrated a bedrock base to them, and there was a large range in depth from 1-26 feet with the average of 8 feet. These sinkholes also ranged in size from 6 to 215 square feet in surface area with averages around 60 square feet. However, there are also many small shallow sinkholes less than two feet in depth and 3 square feet in area. Finally, a Nearest Neighbor Analysis was run on the sinkholes in the area and determined an R value of 0.02 illustrating considerable clustering (Groves et al., 2008).

A technical report, “Geologic Mapping for Water Quality Project in the Upper Iowa River Watershed,” illustrated some interesting findings about sinkholes in that area. By using LiDAR technology, they identified double the amount of sinkholes compared to previous surveying methods. If this holds true, Iowa’s current number of sinkholes will show up as approximately 36,000 using LiDAR techniques (Wolter et al., 2011). The report also concluded that geology played a significant role in the location of sinkholes

within the Dunleith formation and the Galena Group. They illustrated sinkhole density of 19.3 and 13 per square mile, respectively (Wolter et al., 2011).

The historic analysis of sinkholes in Allamakee County was by Palmquist (1977). A simple model was created to determine the environmental and temporal controls of sinkhole development. It was found that sinkholes occurred 5,000 years ago after development of the original surface. Multiple regression analysis indicated that sinkholes formation and propagation were inversely related to local relief and the extent of surface drainage. There was a positive correlation with the Fayette soil and inversely with local relief. The main conclusion was the major control of these sinkholes is the ground water recharge. This also correlates with sinkhole aquifers as the permeability and lithology are important. Other research in Northwest Illinois, Southwest Wisconsin, and Southeast Minnesota can also be linked to Northeast Iowa since it deals with the same geologic groups and formations (Anderson, 1998). This area is also considered to be the driftless region that has not been impacted by recent (Wisconsinan or Illinoian) glacial advances (Prior, 1991).

CHAPTER 3

STUDY AREA AND METHODOLOGY

Study Area

This study involves two research stages. The first stage is to develop and assess LiDAR-based methodologies of detecting karst features and two smaller sites used to test extraction methods are labeled study area 1 and 2 as study sites. The second part of this study focuses on the analysis of sinkhole distribution, characteristics, and typology and focuses on the entire area of the nine counties in Northeast Iowa.

The study area includes nine counties in Northeast Iowa: Howard, Winneshiek, Allamakee, Clayton, Fayette, Delaware, Dubuque, Jackson and, Jones (Figure 3). The total area of these counties is 5,769 square miles in size. It spans a distance of 107 miles from north to south and 122 miles east to west at its greatest points. The area is known to be a scenic area within Iowa as its elevation change is much greater than in other areas of the state, with increasing elevation variability towards the Mississippi river (Prior, 1991). The change in elevation is 738 feet throughout the study area with 1440 feet in Howard County to a low of 702 feet in Jackson County. This region is also heavily vegetated compared to the rest of the state due to the dramatic elevation change limiting row crop farming.

Two representative study areas in Iowa, roughly two square miles in size, were used to complete the first stage. Study area 1 is located just east of the intersection of Locust Road (County road or Highway W38) and Canoe Ridge Road, approximately four

miles north of Decorah Iowa in Winneshiek County (Figure 4). This study area is predominantly farmland and contains approximately ten buildings. Many terraces are found here due to the high relief areas. These high relief areas are known as the driftless region in Iowa as it was not glaciated by the most recent glacial advances allowing the karst region to continue to develop (Groves et al., 2008). This area was selected for several reasons. The first determining factor was this area represented Northeast Iowa's agriculture areas and provides several varieties in shapes of sinkholes. Second, the (DNR) already identified sinkhole locations and boundaries within this area. This allows the possibility of comparing the sinkholes detected using the new method and those identified by DNR. Study area 2 is situated approximately eleven miles north of Dyersville, Iowa. It is located northwest of the White Pine Hollow State Park on DNR land and also within the park itself. The area falls within three counties including Clayton, Delaware, and Dubuque counties (Figure 5). This area is heavily vegetated with a significant degree of elevation change from the bluff to the river valley. The area was selected for several reasons. First, it is a highly vegetated area that has visually discernible sinkholes. At the same time, the DNR has not identified any sinkholes within this study area, and several articles (Seale et al., 2008; Montane, 2001) mentioned that LiDAR was not very accurate or capable of identifying sinkholes in dense vegetation. Finally, this area was easily accessible because the DNR owns the land.

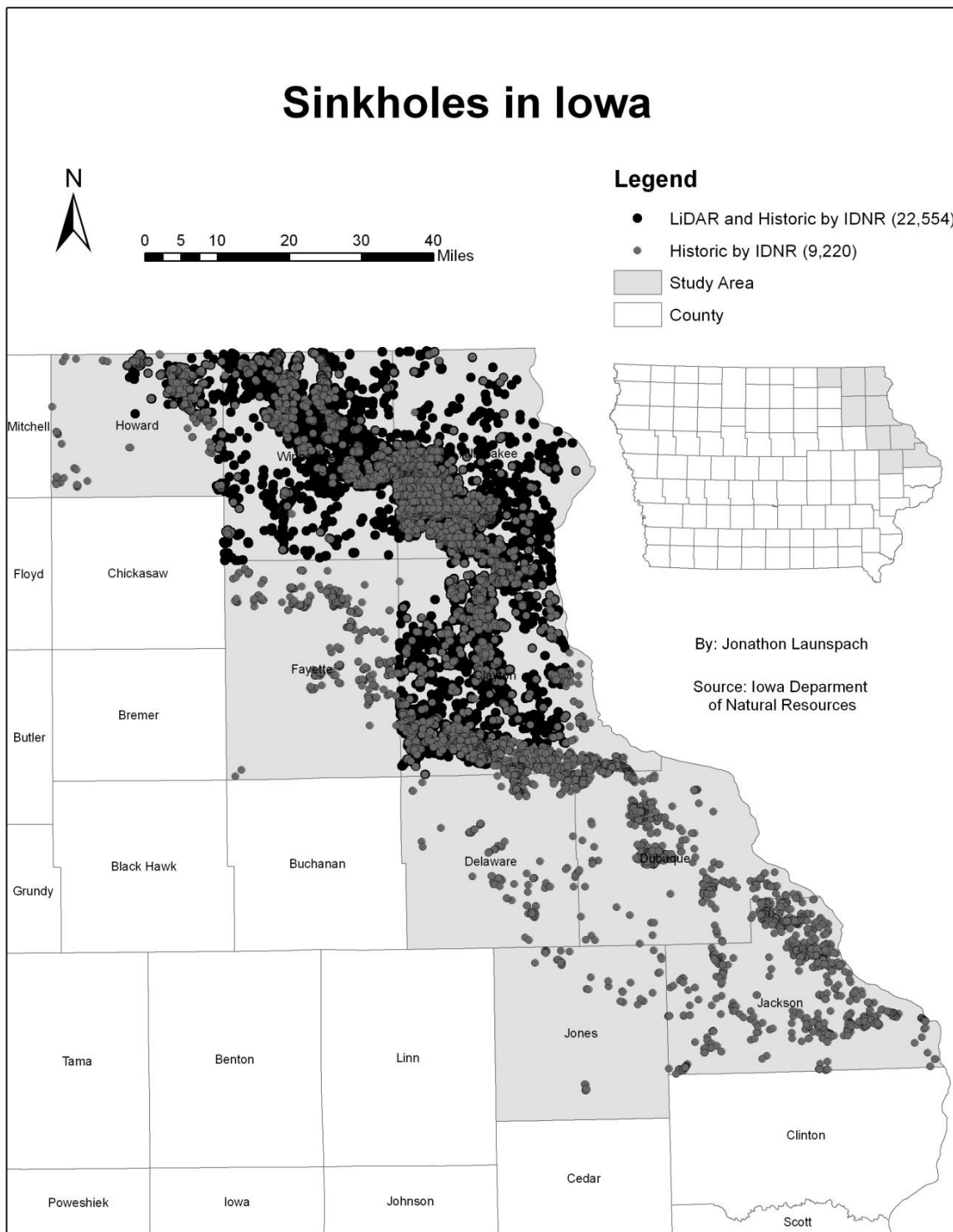


Figure 3: Distribution of sinkholes throughout Iowa based on the DNR; the numbers displayed illustrate the amount of sinkholes within that data set.



Figure 4: A hillshade image of study area 1 allowing visual identification of sinkholes.

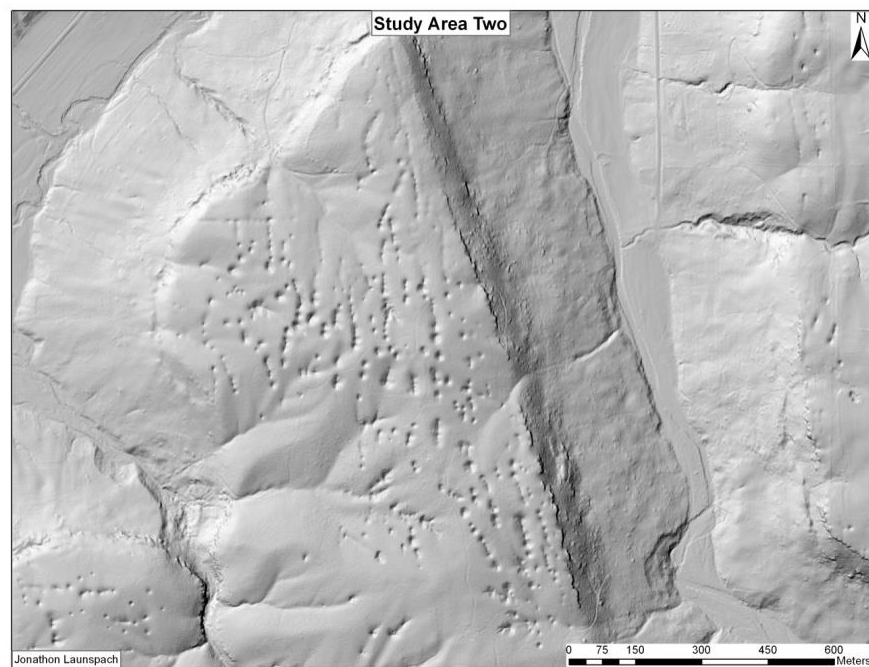


Figure 5: A hillshade image of study area 2 of the dense sinkhole landscape.

Geological Characteristics of the Study Area

The geology of Southeast Minnesota and Northeast Iowa is relatively similar (Gao, Alexander, & Tipping, 2005). The geologic groups and formation mentioned earlier consist of predominately limestone and dolomite that formed mainly within the Ordovician with minor development in the Silurian and Devonian geologic time periods (Anderson, 1983; Figure 6). There are also intermittent layers of shale, and at the bottom of the sequence is a significant amount of Sandstone, which developed during the Cambrian (Anderson, 1998; Groves et al., 2008).

The sinkholes found in Iowa belong to the following geological formations and groups: Galena group and Platteville formation; Hopkinton, Blanding, Tete des Morts, and Mosalem formation; St. Peters Sandstone and Prairie du Chien group; Maquoketa formation; Wapsipinicon group; Cedar Valley group and several others with less significance (Figure 7). All of these units formed approximately 400-475 million years ago (Anderson, 1983). The geological structures consist of vertical joints controlling the flow direction of some streams (Anderson, 1998). More specifically, there are certain geologic formations that allow the development of sinkholes to occur in greater capacity. In particular, these formations are Galena group and Platteville formation, Hopkinton, Blanding, Tete des Morts, and Mosalem Formations (Silurian Formation), which account for approximately 85 percent of the study area in Iowa sinkholes based on IDNR historic data (Anderson, 1998).

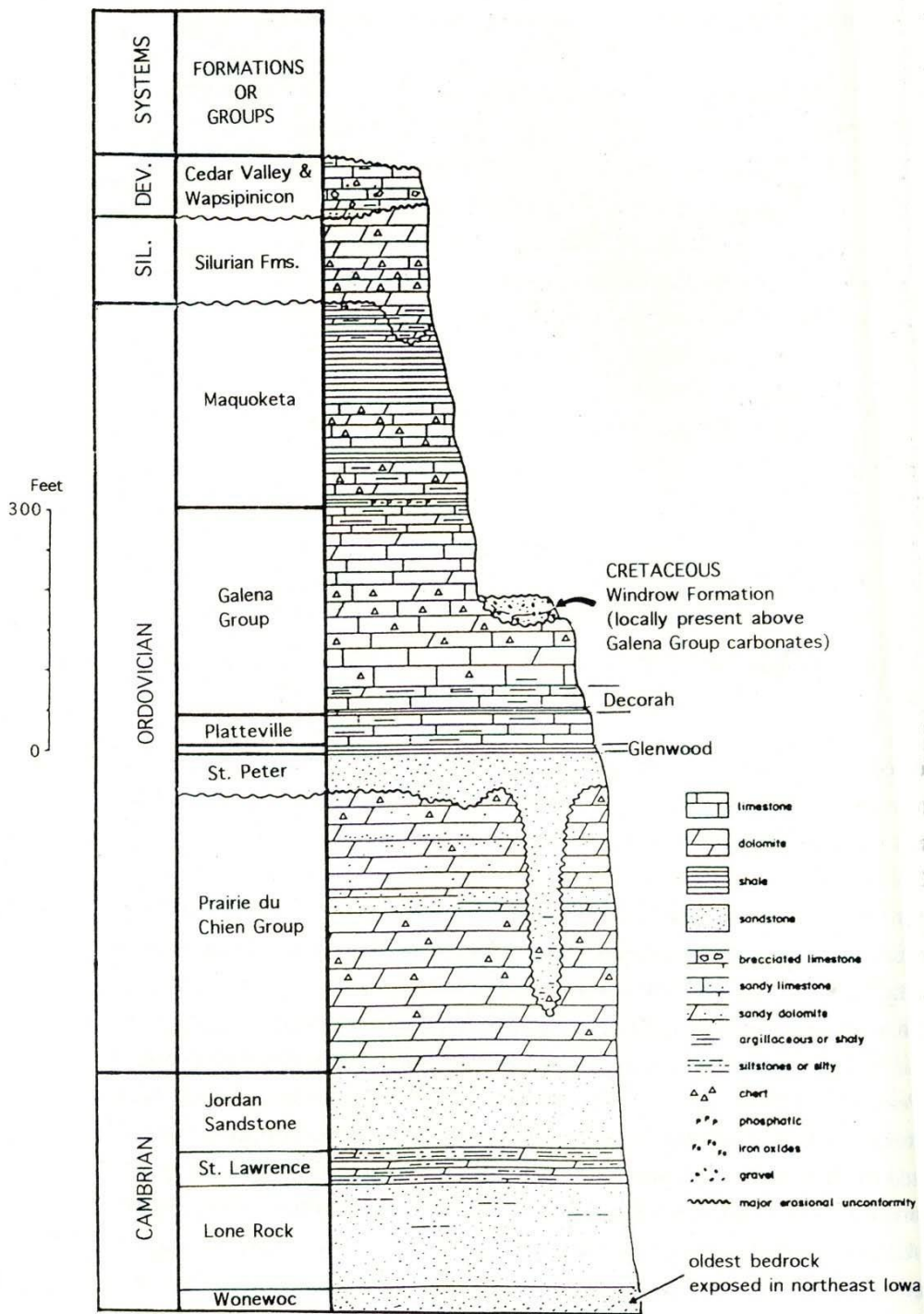


Figure 6: Illustration of the stratigraphic column within Northeast Iowa.

(Anderson, 1998, p. 80).

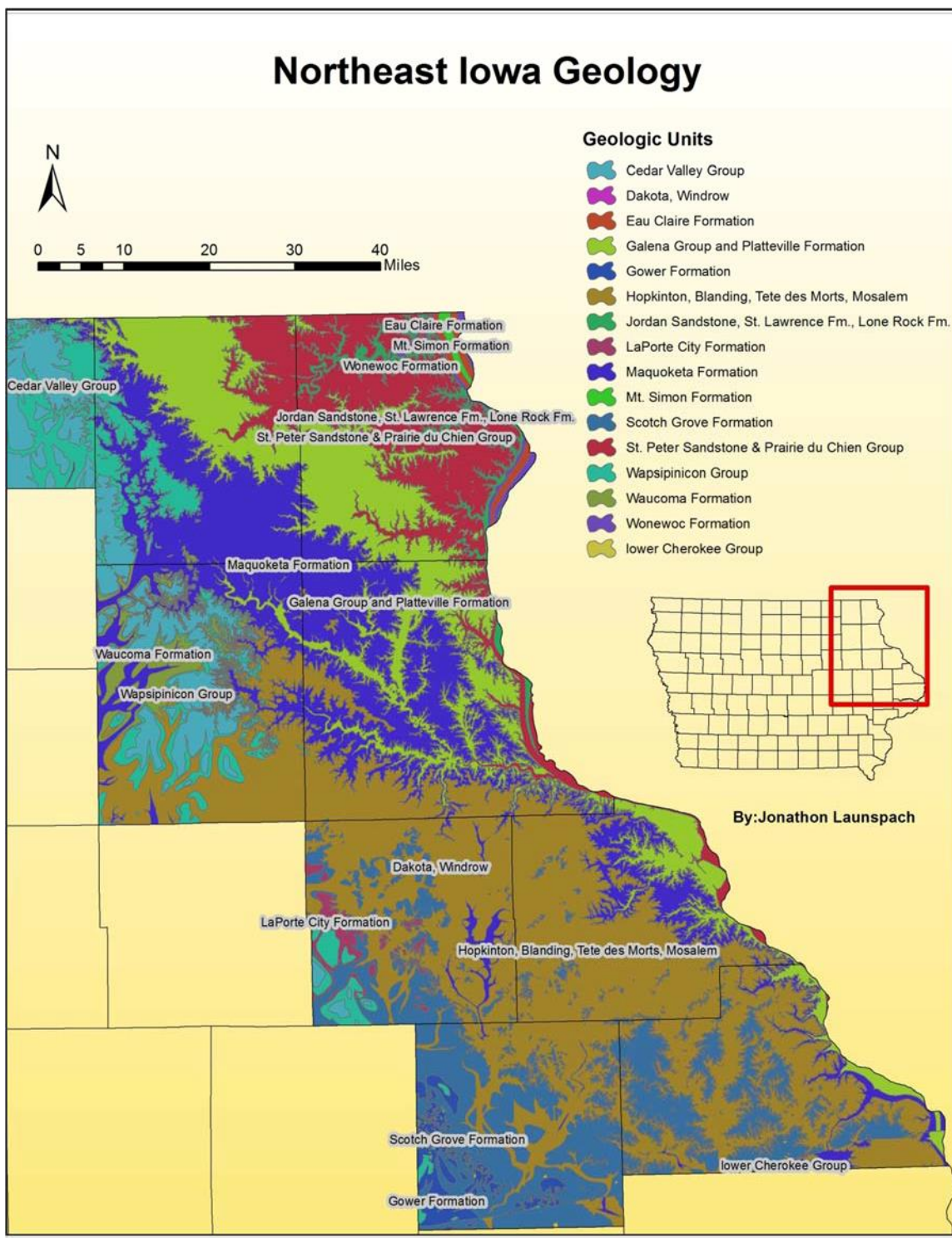


Figure 7: A bedrock geology map of Northeast Iowa; data source IDNR.

Data

LiDAR

The LiDAR data for the small study areas in Iowa was acquired from the GeoInformatics Training, Research, Education, and Extension Center (GeoTree, n.d.) at the University of Northern Iowa. The LiDAR data for the nine counties in Iowa were collected from the IDNR (Table 1) and processed to one-meter resolution (Iowa Lidar Consortium, n.d.) and displays a vertical accuracy is +/- 18 cm. The horizontal accuracy is 1 meter with 1.4 meter average point spacing.

Geologic

Geologic bedrock with the Groups and Formations data were obtained from the IDNR (Witzke, Anderson, & Pope, 2010). Three existing sinkhole datasets were also incorporated into the project. One dataset contains polygons with sinkhole shape area and shape length attributes (Iowa Department of Natural Resources, 2012; Table 1). The other two contain only point locations and identification numbers. All three of these sinkhole datasets have been developed by IDNR (Iowa Department of Natural Resources, 2013).

Physical and Infrastructure Variables

Strahler river order data for perennial streams was collected and developed by the Iowa DNR (Iowa Department of Natural Resources & Geological Survey Bureau, 2000). The original statewide dataset was clipped to the boundary of the study region. The rivers were ordered one through six within the study area and presented as vector lines. The road layer was derived from the Iowa DNR GIS website in the form of vector lines (Iowa

Department of Transportation, 2007). The data was also clipped from statewide data to the boundaries of the study area. Urban areas were also implemented into the model as they were delineated by vector boundaries and clipped by the study area (U.S. Department of Commerce & U.S. Census Bureau-Geography Division, 2010). A 15x15 meter raster land cover dataset was created by the Iowa DNR was also incorporated (Iowa Department of Natural Resources & Geological Survey Bureau, 2008). The land cover data set was classified into 12 different categories. The categories consist of: background, water and wetlands, forest, grassland, cropland, urban and barren, no data, persistent water and wetland, persistent forest, persistent grassland, persistent cropland, persistent urban and barren, and very persistent grassland. Bing Imagery through ArcGIS was also utilized to identify sinkhole location and other possible questionable features, to help aid in visual identification. All of the data that was utilized within the study was projected in Universal Transvers Mercator, Zone 15 North by the Iowa DNR. All of the data was clipped to the study area size.

Table 1: *List of data used and their sources*

Iowa Data	Source
LiDAR	GeoTREE
LiDAR	Iowa Department of Natural Resources
Geologic units	Iowa Department of Natural Resources
GIS Sinkhole layers	Iowa Department of Natural Resources
Aerial photos	Bing Imagery
Strahler river order	Iowa Department of Natural Resources
Road layer	Iowa Department of Natural Resources
Urban areas	Iowa Department of Natural Resources
Land cover	Iowa Department of Natural Resources
Slope 30 meter	Iowa Department of Natural Resources

Field Data Collection

A field survey was conducted within the two small study sites to assess the accuracy of the automated model. The field survey involved the measurement of 73 sinkholes. The sinkhole data were measured using a Trimble GeoXH 6000 Series GPS unit. TerraSync software was utilized to assemble the data and transfer it into ArcGIS. The sinkhole data collection occurred in late October and early November when the tree foliage was a minimum and crops were removed from the field to allow the most access to collect accurate GPS coordinates. A relatively small number of sinkholes were collected from Study Area 1 due to the lack of access to certain private properties. However, it was essential to collect these data in order to be able to complete a cross check between the newly developed model, DNR data, and ground data (Figure 10, Figure 11). The majority of the ground truth data for accuracy assessment was collected in Study Area 2 (Figure 8, Figure 9). The data acquisition in this area was easier since the

sinkholes were primarily located on the DNR owned land. Furthermore, The DNR had not identified any sinkholes at this location, therefore determining the accuracy of field data for my model was used.



Figure 8: Study area 2 showing the general topography of the region.



Figure 9: A sinkhole in study area 2, photographed during GPS boundary measurement.



Figure 10: An Uvala formation in study area 2.



Figure 11: A major sinkhole in study area 1 and surrounding farm field.

Data Processing

The LiDAR data were used to develop a digital elevation model (DEM) of the test study areas. This DEM was created within the ArcGIS 10.1 environment. The first step of the analysis was to examine the existing DNR sinkhole data and three LiDAR-based sinkhole extraction methods to assess their accuracy. This was done on the two testing sites representative of the larger study area. The accuracy assessment was conducted through ground truthing and aerial photo interpretation, as well as DNR data, where available. Field surveys and airborne imagery are crucial to this process as it ensures that sinkholes have been properly identified and mapped (Seale et al., 2008).

The LiDAR dataset was created within ArcGIS utilizing two tools. The first tool can be found within the *3D Analyst Tools*, under Conversion from File. It is called *ASCII*

to *Feature Class*. Parameters that were set within this were one meter resolution with 1.4 meter point spacing (based on the IDNR measurements). Once the first tool had finished processing, an interpolation was conducted using the *Inverse Distance Weighted (IDW)* method in order to create the elevation surface map (DEM). The interpolated elevation was assigned to each pixel.

In order to handle complex geoprocessing operations, further processing was implemented in the ArcGIS Model Builder. DEM data from the two test study sites were processed using three different methods to identify the best sinkhole identification model that would be applied on the entire study area. The three methods tested in this study were: (1) using *Fill* and *Slope* (first derivative) to determine enclosed areas and define sinkhole boundaries; (2) utilizing the slopes second derivative; and (3) using an object-oriented technique (using the eCognition software) derived from remotely sensed data, allowing the capability to extract features (Chen, Su, Li, & Sun, 2009). GIS software was employed to perform the spatial extractions. The methods were tested against the already derived polygon and point sinkhole locations available from the DNR (site 1) and field ground truth data (site 2). Aerial photos provided by the DNR and Bing Maps Aerial imagery were used to assess the accuracy of the derived sinkholes. The most accurate LiDAR-based sinkhole extraction technique or combination of techniques was applied to the entire study area.

Sinkhole Identification Methodology

The large mosaic LiDAR data were acquired from the Iowa DNR. These LiDAR data were partitioned into sections, which ranged in a variety of sizes, for processing. The sizes varied from half a county to a county in size. Altogether, 22 sections made up the entire study area. Although these multi-tile sections overlapped slightly, it was possible to remove overlaps by using the *Dissolve tool* in ArcGIS.

The next step was to assign the correct coordinate system and projection. The system that is used by the Iowa DNR is Universal Transvers Mercator, Zone 15 North. Once all data for Iowa sections of the study area were projected in the correct coordinate system, the next step was to implement them into the model.

Automated Identification Model for Sinkholes (AIMSINK)

The Automated Identification Model for Sinkholes (AIMSINK) developed in this study includes six submodels. The submodels are portions of the entire models that deal with a particular geoprocessing task..

Submodel 1: Slope Extraction

The first stage of the model consisted of two main processes. First was to extract slope from the DEM and the second was to utilize the *Fill tool* to identify sinkholes (Figure 12, Figure 13). The *Slope tool* was run over the study area. Based on literature (Hyland et al., 2005) and from testing 322 sinkholes, it was determined that an angle of 15 degrees or higher would yield the slope of a sinkhole. The *Reclassify tool* was used to classify areas of greater than 15 degrees, and then *Majority Filter tool* was employed

several times to help remove the remaining random isolated pixels, leaving large areas with slope greater than 15 degrees remaining.

Submodel 2: Filling Closed Depressions

The *Fill tool* was then applied to identify the sinkholes (Figure 12, Figure 13). It was a tool derived by Tarboton, Bras and Rodriguez–Iturbe (1991) which has since been implemented into ArcGIS tools. This tool takes into account several of the hydrologic tools in ArcGIS (*Focal Flow, Flow Direction, Sink, Watershed, and Zonal Fill*) to identify characteristics of closed depressions. The raster calculator was then used to subtract the new filled layer from the original layer in order to determine where the sinkholes were located. Next the *Reclassify tool* was used to identify only the values greater than zero or any areas that were filled.

Submodel 3: Combining Fill and Slope to Identify Sinkhole Boundaries

The key to this model is the combination between the fill and slope functions. By taking the two classified raster layers, fill with greater than 15 degrees set to one and remaining dataset to zero, and slope area greater than one set to two and remain dataset to zero, and combining them together will result in the high probability of determining the location of a sinkhole. To extract the sinkhole boundary a sum of the two layers was computed (layer 1 = Fill classified as 1) + (layer 2 = Slope classified as 2) which would add up to three, identifying the sinkholes. However, the actual sinkhole boundary is on average slightly larger, therefore a larger area must be selected (because the fill tool only fills to the lowest elevation, and in many cases this isn't appropriate sinkhole perimeter). To do this the raster layer was converted to vector. The vector layer then had values of

zero meaning no data, one meaning fill, two meaning slope, and three meaning the combination between fill and slope. *The Select by Attribute tool* was used to select combination layer. *The Select by Location tool* was implemented to identify any boundary that intersects with the combined fill and slope layer. This layer was then added to it creating a much more representative depiction of the sinkhole boundary making it slightly larger. From here, the selected regions were converted back to raster and then back to vector to create one single attribute boundary (Figure 12, Figure 14).

Submodel 4: Calculating Sinkholes Area and Axes

In order to remove area of false identification of sinkholes, further methods were applied. First, the three following tools were applied: a *Smoothing tool* to better represent the curvature of the perimeter of the sinkhole and to remove the angulation of each of the polygons. That was followed by a calculation of area for all the sinkholes. Finally, the third tool used was the *Minimum Boundary Triangulation tool* created by Charlie Frye (Minimum Bounding Rectangle [MBR] Analysis tools, 2008). This tool essentially identifies if a shape is lineated or spherical. It calculates the two axes of the polygon and then assigns a ratio value to that sinkhole (Figure 12, Figure 14). In this case, features with the ratio value of 4.0 or less, which means four lengths to one width, would still be identified as sinkholes. This threshold was used because all 685 LiDAR identified sinkholes in both test study areas fell under the ratio of 4.

Submodel 5: Eliminating Non-Sinkhole Features

Several types of depressions found in the landscape can be misclassified as a sinkhole; these include: road ditches, bridges, urban areas, farmsteads, quarries, etc. Therefore some elimination procedures were used to remove the polygons that are not sinkholes (Figure 12, Figure 14). First, the *Selection by Attribute* was used to identify polygon areas, in this case between 12 square meters and 12,000 square meters. These parameters were determined by examining 563 sinkholes in the test study areas. Next, a *Select by Attribute* was used to select those polygons that had length and width axis ratio greater or equal to 4.0. That method removed all large and linear segments, such as linear slivers along roads. The next step was to remove other areas, such as roads and urban zones. Urban areas are problematic and a previous study illustrated that the accurate identification of sinkholes in urbanized landscapes is difficult due to noise from building, over passes, retention ponds and other features (Seale et al., 2008). Roads were buffered at 120 meters. The buffer was determined using a random sampling of 60 roads in Northeast Iowa. The 120 meters covers from the ditch on one side across the road to the ditch on the other side. This was done to eliminate any ditches being identified as sinkholes. The urban areas were then merged to the road layer in a sub selection to create an urban layer. This layer was then removed from the selection to help identify the possible sinkhole locations.

As the majority of sinkholes in Iowa occur in upland areas, to remove river valleys a Strahler river order classification was used. The first order perennial streams were buffered at 20 meters, second order by 40 meters, third order by 60 meters, fourth

order by 80, fifth order by 100 and sixth order by 120 meters. This layer was then removed from selection.

Outside of Model: Additional Elimination of Non-Sinkhole Features

The main model tries to identify sinkholes and their boundaries, as well as determine the boundary of the sinkholes using an automated technique of primarily two tools. There were some selected areas that did not contain sinkholes, therefore the geology layer was used to identify the more likely geologic units that could produce sinkholes. The sinkholes that fell within these geologic units were selected utilizing Intersect tool. A vegetation layer raster was converted to vector and then used to intersect the geology boundaries, to identify main sinkhole-related vegetation types that fall within the geologic units. The sinkholes layer was now derived from the data. The problem, however, was that several areas picked up anthropogenic sinks. These sinks consist of roads, dams, and terrace features that needed to be removed. To do this, a land cover image from the IDNR was utilized to select areas with forest and grass lands, and to remove agriculture areas. The 15-meter resolution image was reclassified into these two categories and then converted to vector. It was then intersected with the sinkhole layer. This process was tested on a random sample of 300 sinkholes before it was implemented into the model. Next, the Iowa DNR data illustrated that 85 percent of sinkholes fall within two geologic units (Figures 6, Figure 7). Therefore, a selection of the top three geologic units was identified as having the most sinkholes was used. These three regions were then intersected with the sinkhole layer. These boundaries identified were then employed back into the model. The remaining selected features are then input into the

Eliminate polygon tool that removes any holes within the polygon layer, creating one uniform layer. The layer is the vector layer that contains final sinkhole boundaries.

Submodel 6: Extracting DEM Data for Identified Sinkholes

After sinkhole boundaries were identified, the next task was to obtain information on sinkhole volume and other geomorphological characteristics (Figure 12, Figure 14). For this purpose, the final layer was utilized to extract the original elevation data to confirm the boundaries of sinkholes, so that all parts of the sinkhole are obtained.

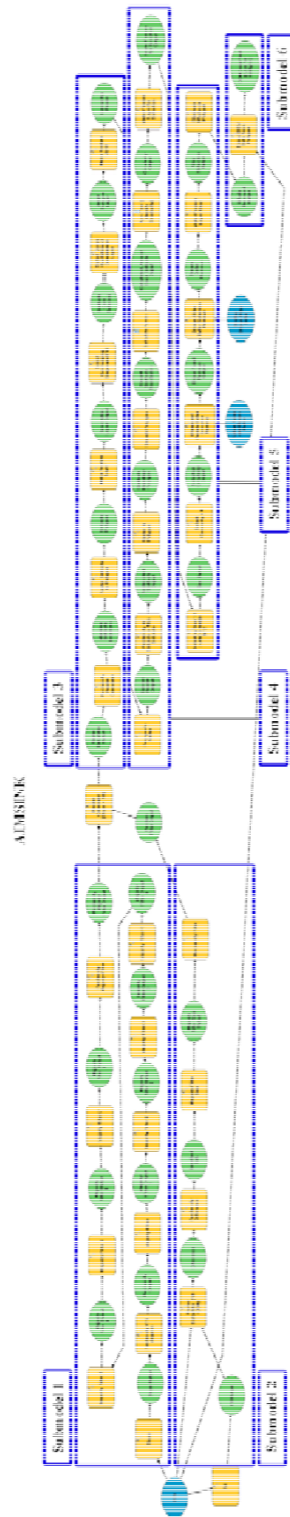


Figure 12: The Completed AIMSINK model.

AIMSINK

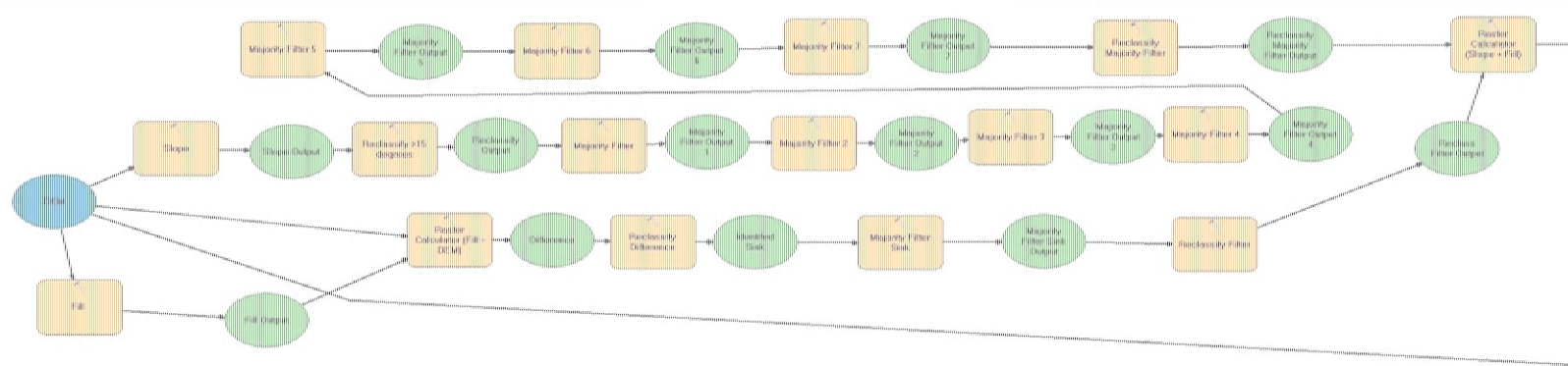


Figure 13: Left side of model.

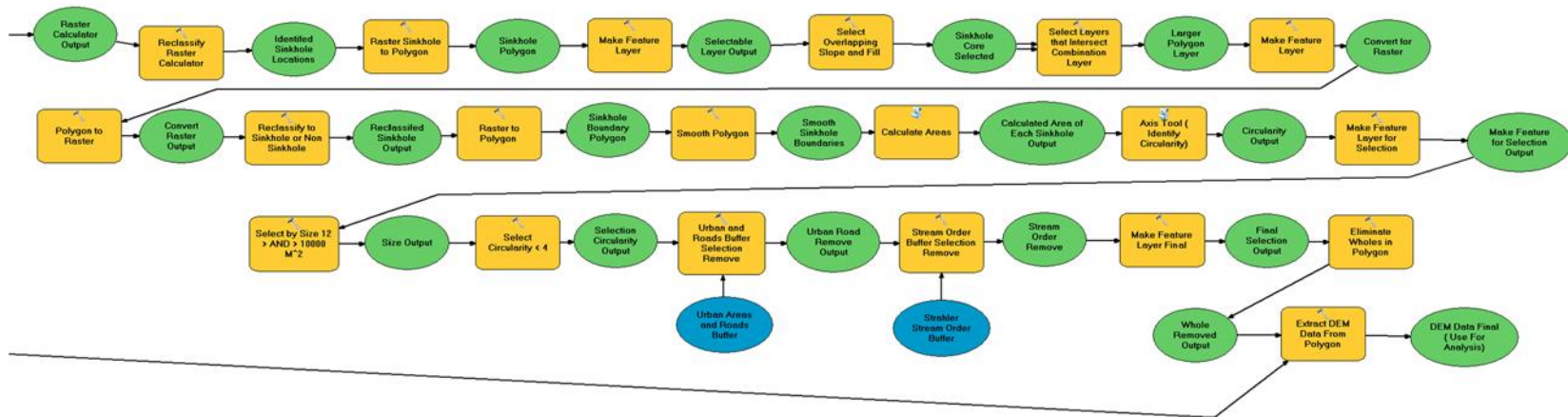


Figure 14: Right side of model.

Accuracy Assessment Methods

Accuracy assessment was implemented on four different tiles; one-tile comprising of site 1 and three tiles (accounting for all GPS locations) comprising of study site 2. The accuracy assessment was based on the ground truth information that consisted of already identified sinkholes by the Iowa DNR (which was done manually through heads-up digitizing), GPS coordinate locations collected in the field, and aerial imagery.

Preparing Features for Geomorphological Analysis

Further analysis examined morphology and possible genesis of sinkholes using quantitative characteristics derived from the LiDAR-based sinkhole maps. The geomorphological characteristics computed for further analysis consisted of: area, perimeter, width and length of axis, depth, geology, relative slope, and distance to river. The axes were already derived from the AIMSINK model and the area and perimeter were created in the attribute table and calculated utilizing the calculate geometry function. Geology layer was identified by means of the Intersect tool.

Distance to rivers was determined by selecting first and second order perennial streams from the Strahler river order method in Northeast Iowa. The Extract by Mask tool was used to define the boundary of the study area. The analysis of 300 sampled sinkholes showed that the streams of high order do not influence sinkholes, and therefore only first and second order streams were selected utilizing the Near tool within Arc Toolbox.

Relative slope needed to be calculated to identify possible correlations with sinkhole shape. The relative slope is the overall, average slope of the terrain surrounding

the sinkholes. A 30-meter resolution DEM was collected from the DNR website. The lower resolution DEM was too coarse to represent most sinkholes and other local topographic features. Therefore this DEM represented the average overall slope of the area. The Extract by Mask tool was used to define the boundary of the study area. The Slope tool was then used to determine the relative slope. In order to determine the prevailing slope, the sinkhole polygons derived from the model were converted to point locations. Then, it is possible to use the *Sample tool*. This provides the common slope in which the sinkhole is found and then adds it to the attribute table.

The procedure used to calculate sinkhole depth consisted of several steps. First, the sinkhole elevation data was Extracted by Mask from a multi-tile 1 m DEM (Figure 11, Figure13, submodel 5). The elevation data were then mosaiced together and the Fill tool was run to estimate the highest elevation of the sinkhole. To ensure that the fill operation produced the output that reached the boundaries created by the AIMSINK model, ten centimeters was added to reach the appropriate height. This was the minimum amount that could be added, based on the test study areas. Once the appropriate depth was identified, zonal statistics were implemented to calculate the maximum depth based on the sinkhole boundary layer derived from the model.

Location and Geomorphic Analysis Methodology

The first stage of the analysis considered the relationships among sinkhole variables (area, perimeter, width, length, ratio, depth) and the location variables (distance to river, relative slope and geology). Correlation analysis was used to reveal these associations. In addition to the correlation analysis, the principal components analysis

method (PCA) was utilized to better understand the covariance among the variables. Finally, the k-means clustering method was employed to determine the typological groups of sinkholes based on multiple characteristics (Field, 2005).

Spatial analysis component of the study addressed two major questions. First, it considered whether the locations of sinkholes exhibit spatial pattern, and more specifically, whether they are clustered in space. Secondly, the analysis was performed to identify whether geomorphological characteristics of sinkholes (sinkhole geometric variables and location variables) demonstrate spatial clustering. Spatial clustering was examined using standard nearest neighbor analysis (Ebdon, 1985) and Ripley's K (Boots & Getis, 1988) based on comparing mean observed distance between nearest points to the expected random distribution.

The next part of the analysis considered whether sinkholes with similar geomorphological characteristics tend to locate next to each other. Global and local Moran's I (Anselin, 1995) and a Getis-Ord G (Getis & Ord, 1992) global coefficient (also known as the 'hot spot' analysis) was calculated for each individual sinkhole to show whether a given geomorphological characteristic is similar or different from its neighbors. The z score and p value represent the statistical significance of the input values.

Anselin Local Moran's I (also known as LISA – local indicators of spatial association) is an autocorrelation analysis method that takes into account the location of input sinkhole features and the input field (perimeter, area, width, length, ratio, depth, etc.). Based on these parameters, it identifies any spatial clusters of similar (positive

autocorrelation) or dissimilar (negative autocorrelation) values. It then classifies all observations that demonstrate significant autocorrelation with their neighbors into four groups. HH, which is, identifies statistically significant (.05 level) clusters of high values. It also recognizes statistically significant values of (.05 level) clusters of low values LL. For example, if sinkholes with large area are clustered near each other, such occurrence will be labeled as HH; conversely, a cluster of sinkholes with small areas will be designated as LL. Another group will be identified as HL grouping high values with features of low values. The final group is clustering low values with features of high values LH. Inverse distance was utilized for the type of conceptualization of spatial relationship; this was run on both the geometric variables and the locational variables. Inverse distance weighted considers neighbors of all features; however, closer features in this case are more likely to be associated with their neighbors than further distance neighbors (Anselin, 1995).

Hotspot is similar to LISA in that it assigns weights to features; however, it is a slightly different mathematical calculation that identifies high and low spatial clusters. High values may be determined, but not identified as a hotspot (Ord & Getis, 1995). In order to be identified, all high values must be clustered together. The local sum of the features is then compared to the total of all the features. When the sum is different from the expected, then it assigns a value and determines its significance (Getis & Ord, 1992).

CHAPTER 4

RESULTS AND DISCUSSION

AIMSINK Results and Accuracy Assessment

AIMSINK model as described in the previous chapter (Figure 12) was applied to a section of Northeast Iowa comprised of nine counties (Allamakee, Clayton, Delaware, Dubuque, Fayette, Howard, Jackson, Jones, and Winneshiek). The model identified 47,445 sinkholes in this study area (Figure 15). The sinkholes are present in all nine counties with bands of higher concentration in several parts of this region.

Accuracy assessment of the AIMSINK method was conducted using two test study sites. The ground-truth data used were the sinkholes digitized by Iowa DNR, GPS coordinate locations collected in the field, and analysis of digital aerial imagery (Figure 16). The results for study area 1, demonstrate AIMSINK accuracy at 100% with GPS data, 97% with DNR data, and 88% with the results of visual examination and air photo analysis (Table 2). Unfortunately, the Iowa DNR has not published a formal accuracy assessment of their sinkhole layer; only visual identification based on aerial photos as well as some ground truthing has been performed (IDNR, 2012). In addition, the DNR dataset also includes historic sinkholes that may not be relevant to current LiDAR extraction techniques, because some of the sinkholes have been filled in or altered since they were identified. Study area 2 illustrated 99% accuracy of the model when comparing identification of sinkholes with those collected using GPS and 96% compared with visual analysis (Table 2).

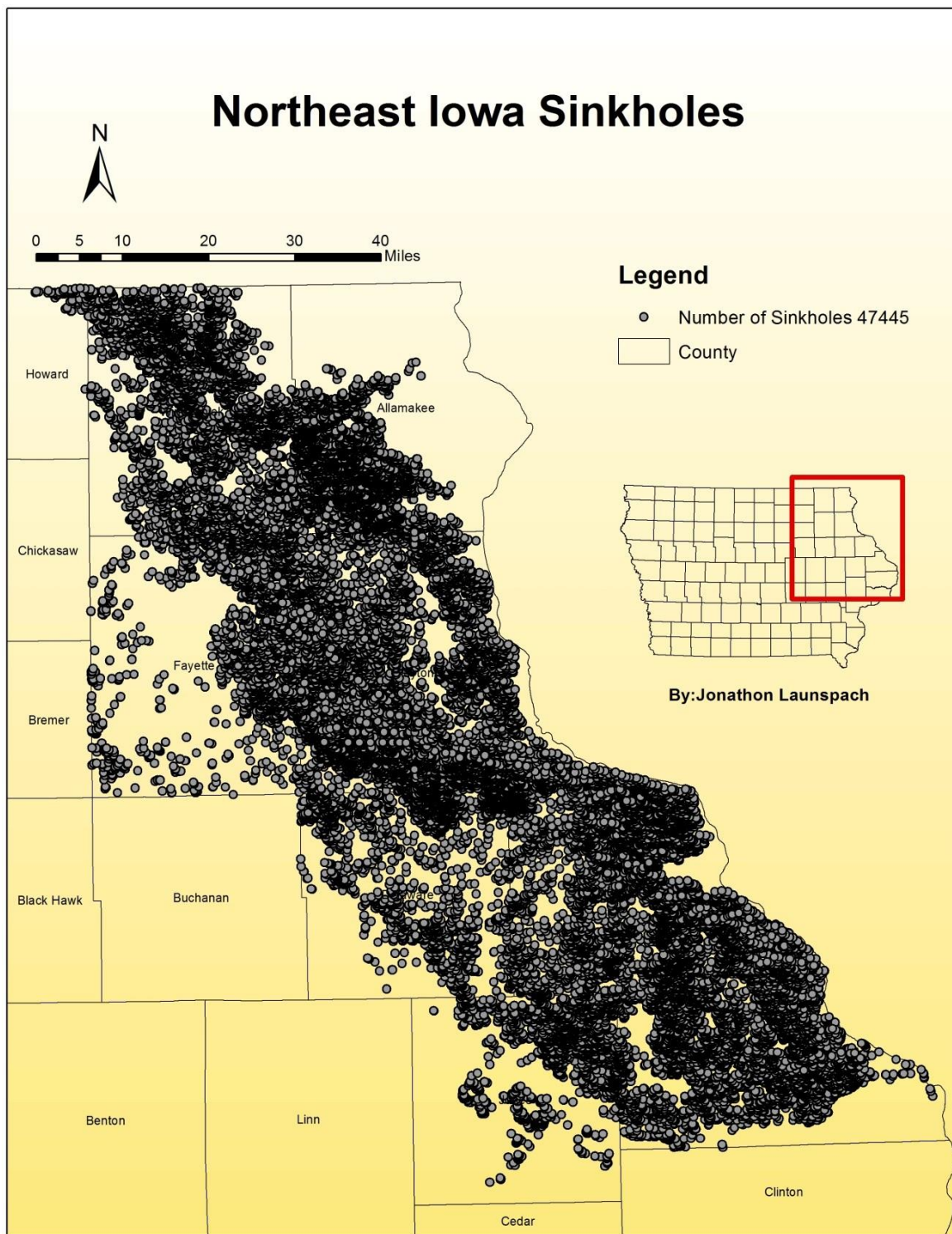


Figure 15: A Map of 47,445 sinkholes identified by the AIMSINK model.

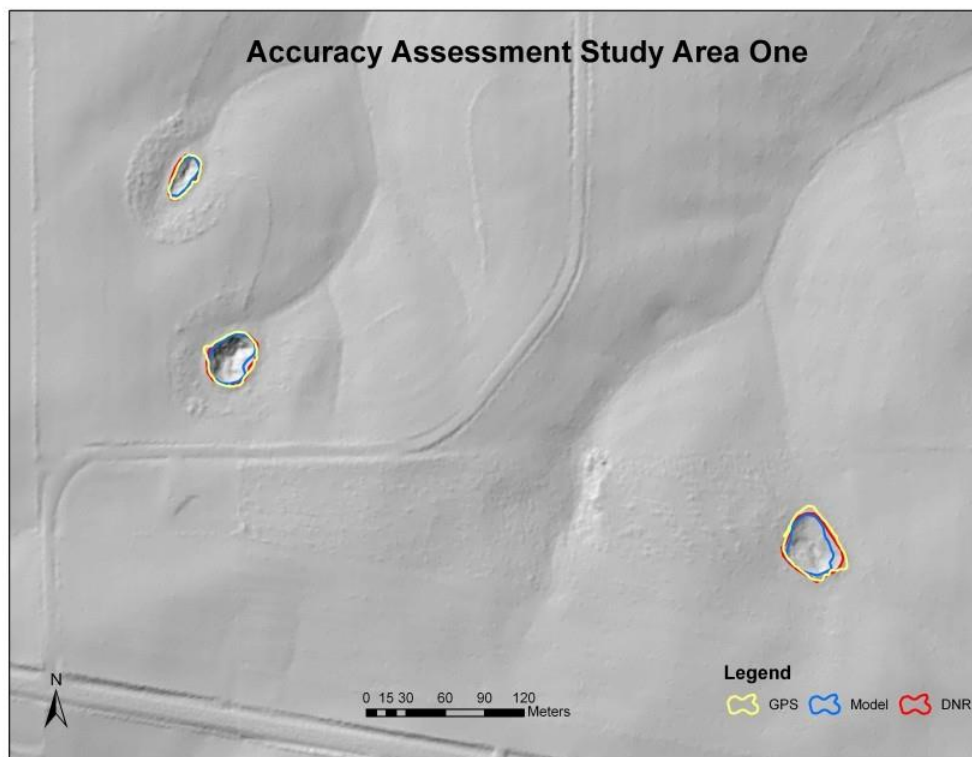


Figure 16: The image illustrates the accuracy of three sinkholes utilizing three different techniques. Yellow represents the boundary that was collected using GPS. Blue represents the boundary of the AIMSINK model and Red represents the boundary of the heads up digitizing the Iowa DNR produced based on the LiDAR data.

Table 2:
Accuracy assessment of AIMSINK in two study areas based three methods

Location	Ground truth method	AIMSINK Accuracy	Omission Error	Commission Error
Area1	GPS	100.0 %	0%	0%
	Aerial imagery	88.0%	12.5%	19.5%
	DNR	97.0%	1.0%	19.5%
Area2	GPS	98.6 %	0.6%	0%
	Aerial imagery	96.2%	4.0%	4.9%
	DNR	N/A	N/A	N/A

Statistical Analysis

Statistical Analysis was performed on the entire dataset in SPSS, which included the variables area, perimeter, width, length, ratio, depth, distance to river and slope. Geology was excluded due to the categorical organization of the data. It is hard to incorporate these parameters into a ratio dataset with much larger variations in values.

Further analysis was performed on the seven variables derived from the AIMSINK model. The two types consist of sinkhole geometric (morphological) variables and location variables. These variables were incorporated into the correlation analysis. The correlation matrix demonstrates several significant patterns (Table 3).

Perimeter displayed a positive correlation with shape area, axis width, axis length, and ratio. This is illustrated by the fact that as perimeter gets larger, all planform features (shape area, width, and length) increase. There is a weak, but significant, negative correlation between perimeter and depth showing as the overall planform size increased depth decreases. The correlation between river distance and slope illustrates a positive relationship implying that sinkholes with larger surface areas perimeters develop further away from streams. There is also a weak, but significant, negative correlation between perimeter and regional slope. That relationship shows a slight trend towards larger sinkholes, in the planform, tend to develop on flatter slopes.

The shape area shows positive correlation with the other morphological variables, illustrating as area increases geometric properties will too. There is also a weak, but significant, positive correlation to sinkholes and river distance indicating sinkholes with the larger areas tend to be found further away from rivers. It also displays a minor

negative correlation between slope and area. This implies that area increases at lower slopes.

Width and length, which represent the long and short axes, exhibited similar results with the sinkhole planform variables with slight variation between ratios. The axes ratio represents the sinkhole circularity with one being perfectly circular and large numbers representing elongation. A weak, but significant, negative correlation was found between length and depth, so as sinkholes get longer they tend to stay shallow relative to the overall dimensions.

Ratio is similar to width and length when relating them to sinkhole planform variables. In addition, a weak, but significant, negative correlation between ratio and depth was identified (Table 3). This means that as the ratio increases, depth will decrease. There was also a slight negative correlation with river distance and the ratio. As the ratio increases, the river distance decreases meaning the sinkholes get longer closer to the rivers. A small negative correlation was determined between ratio and slope. As the ratio increases the slope tends to decrease illustrating longer sinkholes are found on flatter surfaces.

The remaining variable illustrates several other key correlations. Depth illustrated a weak, but significant, correlation with rivers showing that depth increases further away from rivers.

Principal-Component Analysis (PCA) was run in SPSS. A factor of rotation was implemented to maximize the dispersion of the loadings between factors. This is done to help understand the covariance of sinkhole characteristics. Three main principal

components were identified between the geometric sinkhole variables and locational variables (Table 4). Component group one consisted of perimeter, area, width, and length (all positive). Component group two was comprised of ratio (negative), depth, and river distance. Component group three contained just slope.

Table 3: *Correlation table of sinkhole variables*

		Perimeter	Shape_Area	Axis_Width	Axis_Length	RatioL2W	Depth	River_Distance	Slope
Perimeter	Pearson Correlation								
	Sig. (2-tailed)								
	N								
Shape_Area	Pearson Correlation	.888(**)							
	Sig. (2-tailed)	0							
	N	47445							
Axis_Width	Pearson Correlation	.914(**)	.914(**)						
	Sig. (2-tailed)	0	0						
	N	47445	47445						
Axis_Length	Pearson Correlation	.957(**)	.886(**)	.896(**)					
	Sig. (2-tailed)	0	0	0					
	N	47445	47445	47445					
RatioL2W	Pearson Correlation	.184(**)	.066(**)	-.026(**)	.294(**)				
	Sig. (2-tailed)	0	0	0	0				
	N	47445	47445	47445	47445				
Depth	Pearson Correlation	-.015(**)	-0.008	-0.002	-.013(**)	-.040(**)			
	Sig. (2-tailed)	0.001	0.102	0.627	0.004	0			
	N	47445	47445	47445	47445	47445			
River_Distance	Pearson Correlation	.082(**)	.103(**)	.116(**)	.092(**)	-.056(**)	.062(**)		
	Sig. (2-tailed)	0	0	0	0	0	0		
	N	47445	47445	47445	47445	47445	47445		
Slope	Pearson Correlation	-.013(**)	-.014(**)	-.018(**)	-.015(**)	-.011(*)	0.002		-0.002
	Sig. (2-tailed)	0.005	0.002	0	0.001	0.013	0.674		0.624
	N	47445	47445	47445	47445	47445	47445		47445

** Correlations that are statistically significant at 0.01 level.

Loadings in group one provided evidence that these geometric (morphological) features that pertain to perimeter and shape all have relation to each other, and thus are likely to exhibit similar behavior. In contrast, depth and shape had heavy loadings on component two (with opposite signs). Depth showed a considerable covariance with distance to rivers. Principal component three contains slope that exhibited little covariance with other variables. PCA results, therefore, identify three latent vectors in sinkhole differentiation: planform geometry, depth and shape, and relative slope.

Table 4: *PCA of sinkhole variables.*

	Rotated Component Matrix (PCA)		
	Component		
	1	2	3
Perimeter	0.973		
Shape_Area	0.951		
Axis_Width	0.958	0.117	
Axis_Length	0.972	-0.119	
RatioL2W	0.166	-0.686	-0.135
Depth		0.511	
River_Distance	0.142	0.605	
Slope			0.988

Extraction Method: Principal Component Analysis.

Rotation Method: Varimax with Kaiser Normalization.

a. Rotation converged in 3 iterations.

K-means cluster is a grouping mechanism that uses multiple characteristics to assign sinkholes to groups with similar geometric properties (i.e. identifies a typology of sinkholes (Field, 2005)). This process was run using a standard algorithm in SPSS. Since preliminary agglomerative cluster analysis was unfeasible due to a very large number of observations, several numbers of original cluster centers were tested in order to identify the most appropriate number of clusters. A five cluster solution was selected. The resultant clusters were then compared to one another to determine their cluster characteristics (Table 5). The first cluster included small, round, and shallow sinkholes with approximately 60% of the sinkholes falling within this group. The second cluster incorporated large and shallow sinkholes with around 1.5% of the sinkholes in this category. The third group recognized medium, deep sinkholes with 11% of the total

number of sinkholes. Cluster four is primarily comprised of small, round, and deep sinkholes with 23% falling within this type. Finally, group five included large/medium sinkholes with shallow depth, accounting for 3.6% of the total sinkholes.

Table 5: *K Means clustering of sinkhole variables broken into five categories.*

	Final Cluster Centers				
	Small, round & shallow	Large & shallow	Medium & deep	Small, round & deep	Larger/ medium & shallow
Perimeter	73.7	1036.2	344.8	96.3	637.2
Shape_Area	229.9	8159.5	2022.4	357.2	4706.7
Axis_Width	12.7	109.9	47.6	16.4	78.1
Axis_Length	26.1	237.8	101.2	32.9	167.1
RatioL2W	2.0	2.2	2.1	2.0	2.2
Depth	0.6	0.6	0.7	0.7	0.6
River_Distance	226.1	478.6	460.2	794.3	479.5
Slope	15.1	14.7	14.8	15.0	14.7
Total	28537	708	5422	11069	1709
Percent of total	60.1%	1.5%	11.4%	23.3%	3.6

Spatial Analysis

Sinkhole Clustering

Nearest Neighbor analysis identified a significant clustering of sinkholes in the study area ($R=.40$, $z\text{-score} = -249$). This method compared mean observed distance between nearest points to the expected random distribution (Boots & Getis, 1988; Ebdon, 1985). Similarly, Ripley's K function illustrated a tendency to cluster (Figure 17). Therefore, both methods provide a strong indication of spatial clusterization among sinkholes themselves. Further analysis will deal with spatial clustering of sinkhole morphological and locational characteristics.

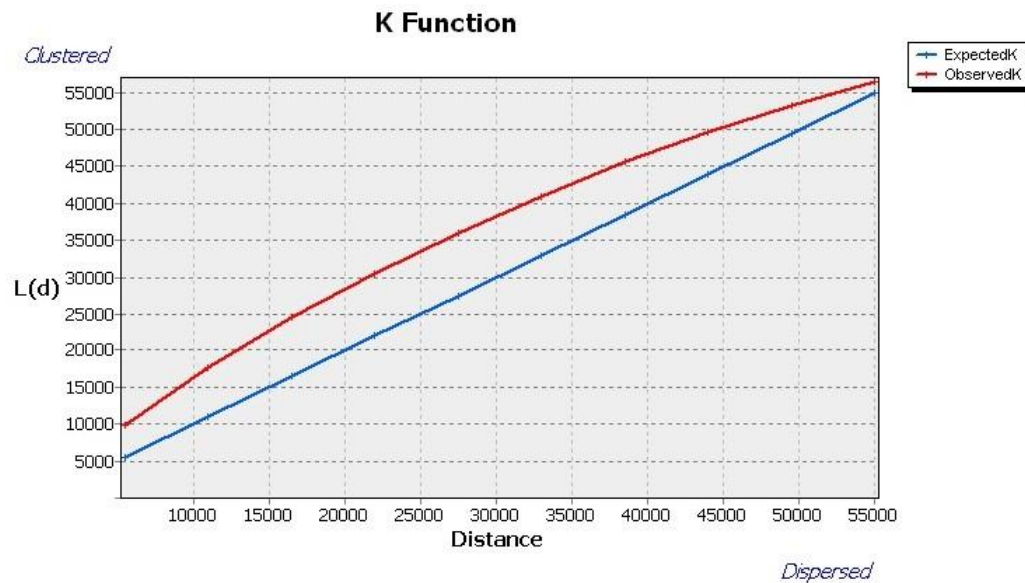


Figure 17: Ripley's K function of entire study area.

Spatial Patterns of Sinkhole Characteristics

Global Moran's I was computed to examine the spatial autocorrelation of sinkhole characteristics in the entire study area. The method standardized spatial autocorrelation by variance in the data set. Table 6 illustrates positive significant spatial autocorrelation among all the variables (Ancelin, 1995). This indicates that sinkholes with similar morphological and locational characteristics tend to cluster. This evidence warrants further analysis of local autocorrelation to identify the clustered regions within the study area.

Table 6: *Global Moran's I of all variables showing clustering of all values.*

Spatial Autocorrelation (Global Moran's I)		
	Moran's Index	Z score
Area	0.0488	49.7
Perimeter	0.0535	54.5
Width	0.0532	54.2
Length	0.0631	64.2
Ratio	0.1555	158.3
Depth	0.1129	115
Dist river	0.0817	83.3
Slope	0.175	178.6

Local Indicators of Spatial Association (LISA) and Hotspot analyses are standard techniques that test spatial autocorrelation of a given variable. In this study these methods were applied to detect the evidence of autocorrelation among geometric and location sinkhole variables, except for geology, due to only three geologic units (Appendix). All of them identify certain clustering patterns of sinkholes; some variables demonstrated more pronounced patterns better than others. Overall, it is evident that sinkholes with similar characteristics exhibit a tendency to cluster in space, a pattern that may be indicative of the influence of certain underlying geological and geomorphic factors. It is, however, difficult to establish more generalized patterns of clusterization that would account for multiple sinkhole properties.

When examining the maps of individual indices, several generalized clusters can be observed. Clusters are identified as C1, C2, C3, C4, C5, C6, and C7 (Table 7, Figure 18). Local Indicators of Spatial Association for area, perimeter, width, and length demonstrate similar characteristics in clusters C2, C4, C5, and C7 which have all four variables with a prevalent HH pattern (High-High, i.e. clustering of high values), Clusters C1, C3 and C6 demonstrate a prevailing HL pattern (High-Low, i.e. negative autocorrelation). The pattern is different, however, when examining ratio between width and length axes. This variable shows HL cluster within C1, C2, C3, and the remaining clusters show similar results with C5 HH, C6 HL, and C7 HH. Depth displays an inverse pattern with C1, C2, C3, C4 merged into HH, C5 HL, C6 HH, and C7 HL. The distance from rivers demonstrates a slight HH clustering in the C1 and C3 regions. Other regions have very little autocorrelation, however some display LL (i.e. clustering of lower values). Finally, relative slope displayed unique results with C1 having HH, C2 None, C3 HL, C4 LL, C5 None, C6 HH, and C7 HH. Sinkhole characteristics that exhibit similar spatial patterns were also found heavily loaded on the same principle components (Table 4, Appendix).

Hotspot Analysis was run on all of the geometric and location sinkhole variables except for geology because of the three geologic units. Again slope, perimeter, length, and width illustrate similar statistically significant patterns (Figure 18). There is slight variation among them, however as a whole, they portray the same results. Circularity (Ratio) demonstrates similar characteristics with positive but less intense clustering in all the clustering groups. There are several locations in groups C3 and C6 where this

variable has a negative standard deviation of z-values. Depth displays high clustering in C1, C2, C3, and C6 with a positive standard deviation of z-values while the remaining regions show little grouping. The distance to river demonstrates little clustering with only region C2 showing some evidences of high standard deviation. Slope demonstrates unique results where the only major clusters are in C4 with negative standard deviation and C6 with positive standard deviation. These results also display similarity among sinkhole characteristics that have high factor loadings on the same principle components in the PCA analysis (Table 4, Appendix).

It is clear, after examining these different clusters, there is autocorrelation among most of the planform variables (area, perimeter, width, and length) as they portray the same results with high-high values and high-low values in certain regions. The circularity has similar, but slightly different, groupings, specifically C2. Depth illustrates the exact opposite of the planform geometric variables i.e. demonstrates low-low autocorrelation in regions where geometric variable exhibit high-high clustering. This can be compared to river distance, which illustrates similar patterns. Based on this, it is clear these areas do portray the same loading factors that were produced by the PCA analysis.

Interestingly, regions C1 through C7 have spatial correspondence with the Geological units. For example, C1- C4 fall within the Galena Group and Platteville Formation; C5-C6 fall with the Maquoketa Formation and C7 falls within the Hopkinton, Blanding, Tete des Morts, and Mosalem. Based on this information one could speculate that the Galena Group and Platteville formation has a lower water table, due to the geologic sequence within the formation, causing the sinkholes to develop at greater

depths. It also displays a relatively high joint system as it was identified by geologists mining for lead and zinc (Anderson, 1998). There may also be localized regions within these formations that cause certain sinkhole variables to develop more prevalently.

Table 7: *The graph displays the sinkhole variable groupings among each region.*

	LISA Analysis Groups						
	C1	C2	C3	C4	C5	C6	C7
Area	HL	HH	HL	HH	HH	HL	HH
Perimeter	HL	HH	HL	HH	HH	HL	HH
Width	HL	HH	HL	HH	HH	HL	HH
Length	HL	HH	HL	HH	HH	HL	HH
Ratio	HL	HL	HL	HH	HH	HL	HH
Depth	HH	HH	HH	HL	HL	HH	HL
River Dist			HH				
Slope	HH		HL	LL		HH	HH

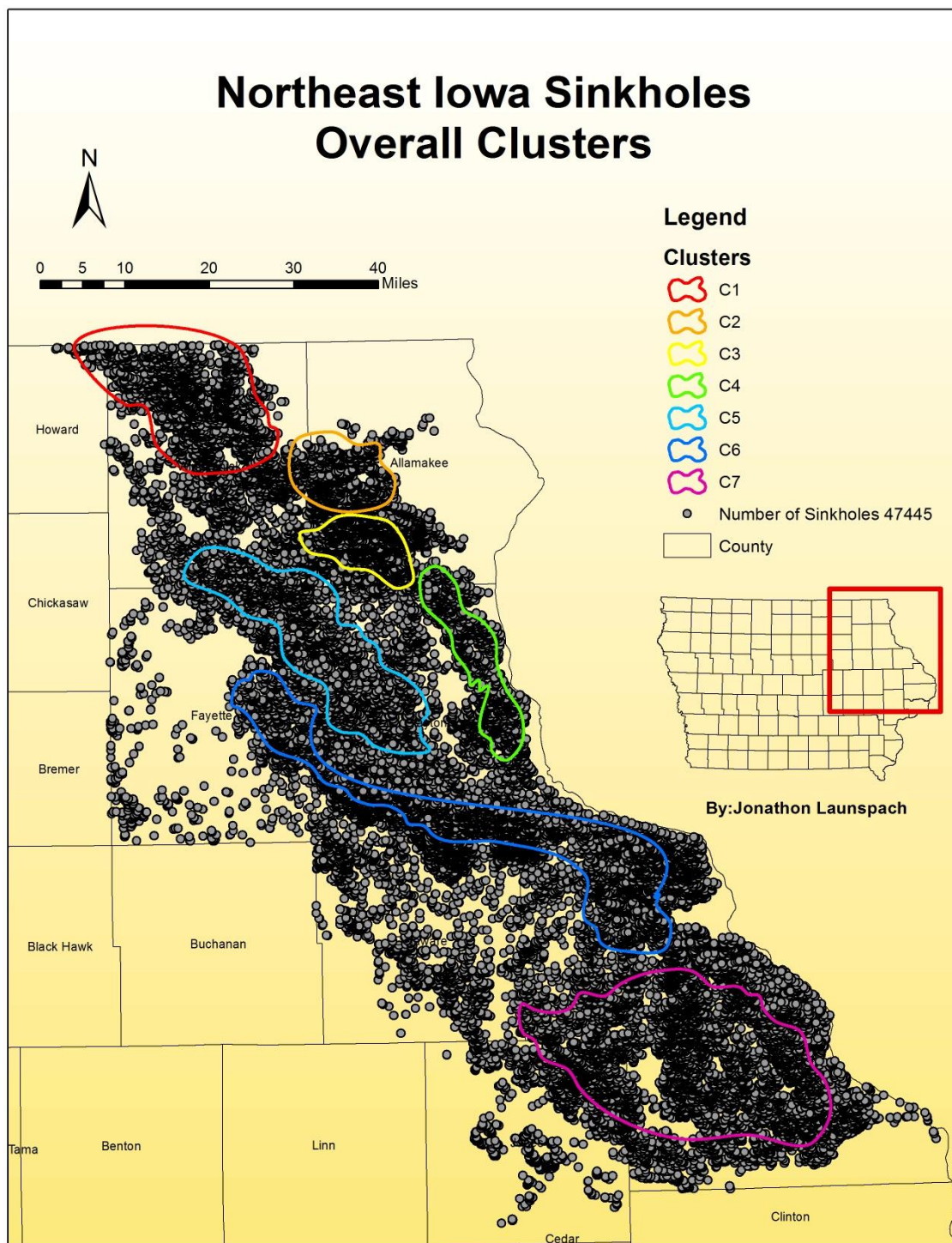


Figure 18: Composite clustering groups from Moran's I and LISA models. See Table 7 for clustering patterns of end groups.

Alternative Methods of Sinkhole Identification Tested in This Study

Object-Oriented Method

An object-oriented classification technique was implemented using remote sensing software titled eCognition. Object-oriented classification is a relatively new technique that has been introduced into the field of remote sensing (Ivits & Koch, 2002). The concept of object-oriented classification is to identify pixels of similar characteristics in the same area instead of basing classification solely on pixel values. In this study, however, it is important to identify sinkholes using several types of inputs. The inputs that were utilized to determine the boundary of the sinkholes included slope, curvature, hillshade, and elevation (Figure 19). However after implementing several eCognition options and combinations of inputs, the results were not accurate (Figure 20). The sinkhole boundaries frequently formed unclosed polygons or produced dissected sinkhole features. The poor accuracy of eCognition results was likely due to a high variability in size and shape of the sinkholes (Glennon, 2010). Future advances in object-oriented classification may provide the ability to identify the boundaries with greater detail and accuracy.

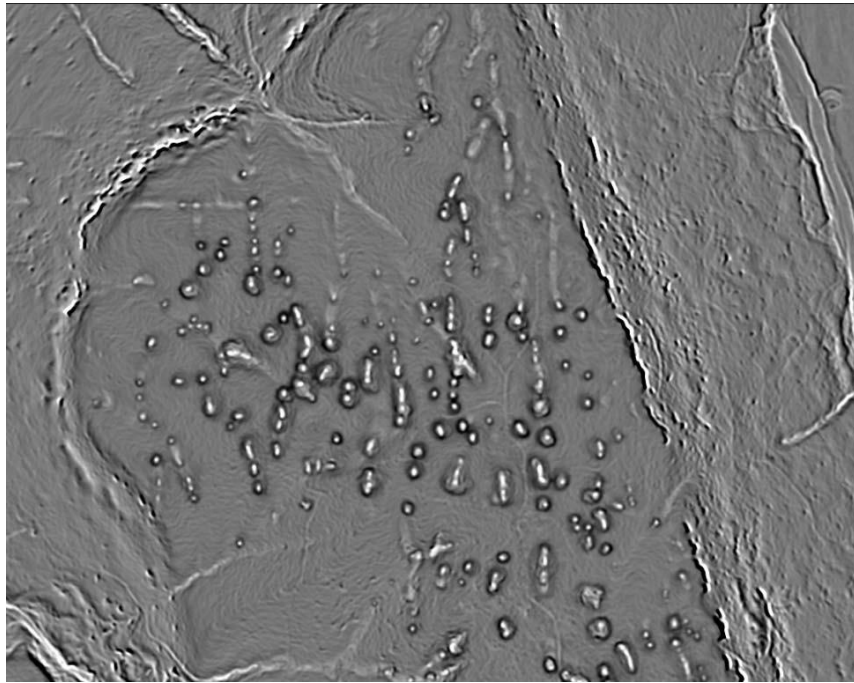


Figure 19: Curvature image that was utilized for object-oriented classification.

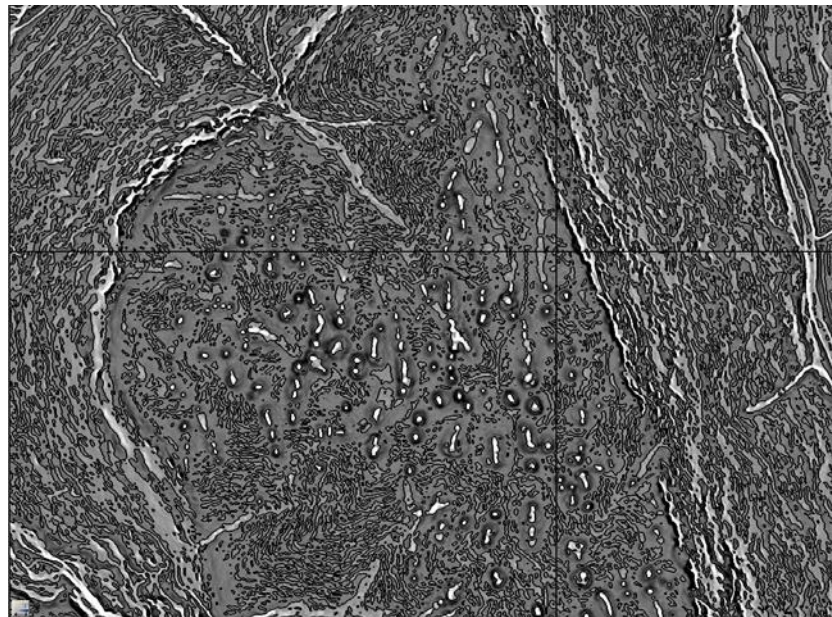


Figure 20: Results from object-oriented classification.

Curvature Method

Slope is a key factor to consider when examining sinkholes. This is because slope has several unique characteristics to consider. One of them is the rate of change of slope. This characteristic is also referred to as the second derivative in most mathematical applications and curvature within ArcGIS (Figure 21). Curvature can be examined in several ways. A profile curvature measures the change in slope vertically, whereas planform curvature examines the change in slope horizontally. Topography also can be examined using curvature, which is an average or combination of two profiles. Applications of these parameters indicate that the curvature does determine sinkholes rather well (Figure 22). More specifically, however, the profile view identifies the boundaries with greater detail. Planform view provided a good understanding of the bottom or deepest part of a sinkhole (Figure 22). Combining these three different parameters can be a powerful tool to identify sinkholes and their boundaries. The major limitation of this method, however, is that many sinkholes do not have a perfect bowl-like shape. Therefore, this method is only reliable if the sinkholes have a continuous concave, approximately circular shape. Because a majority of the sinkholes do not conform to it, this method is challenging to apply (Figure 23). Trying to classify the image proved to be difficult as different types of curvature provides different shapes. For example, a profile view displays a donut shape due to the change in curvature from the top of the sinkhole to the bottom. Slight variations of this occurred within planform and curvature methods, as well as their combinations.

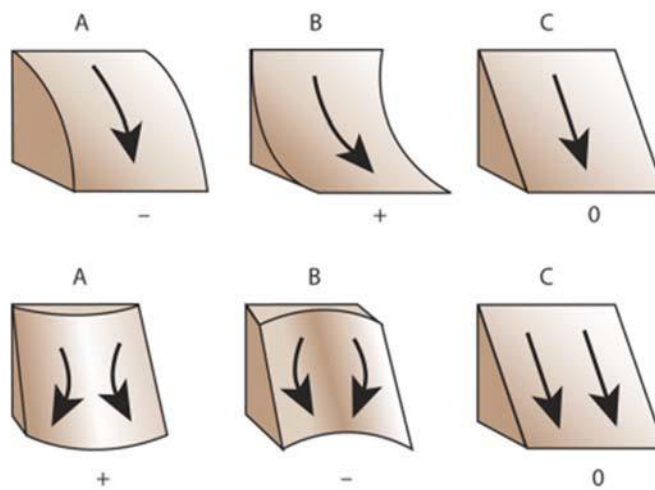


Figure 21: Curvature description of different combinations: The top three shapes represent the difference in values that can be acquired from profile curvature. The bottom three represent the difference in values that can be acquired from profile view. A combination of these can create a curvature output.

(Kimerling, Buckley, Muehrcke, & Muehrcke, 2012, p.360.)

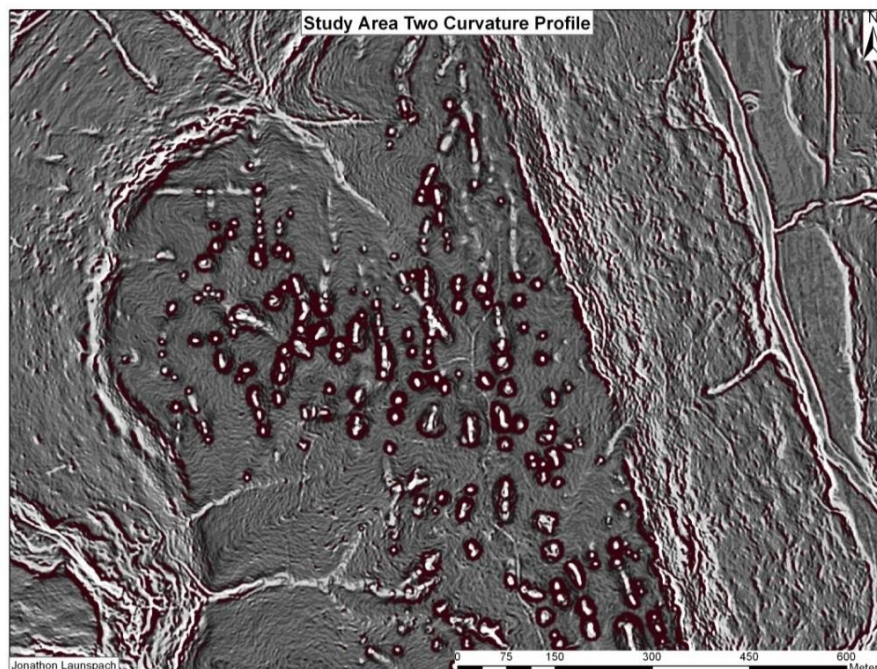


Figure 22: Study Area 2 curvature profile map.

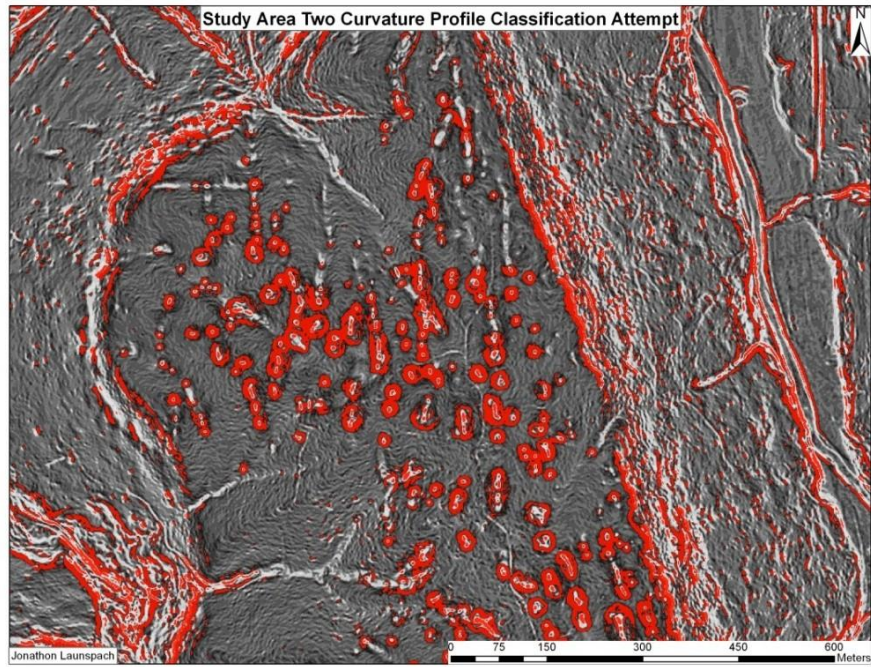


Figure 23: Study Area 2 Curvature profile classification attempt map.

CHAPTER 5

CONCLUSIONS AND LIMITATIONS

Conclusions

The goal of this study was to develop an automated process and assess LiDAR-based methodologies for detecting karst features over a larger area in order to improve understanding of karst distribution and typology in Northeast Iowa.

The AIMSINK Model

This study tested several extraction techniques; however, based on the methods tested (slope, fill, second derivative, and object orientated classification), a combination of slope and fill was determined as the most suitable for the model (AIMSINK). The model was comprised of six submodels. The first two submodels utilized the slope and fill functions to determine possible sinkhole locations. Submodel three merged the fill and slope into a sinkhole polygon layer. Submodel four smooth's the polygon and calculates the area to prepare for submodel five, which eliminates the non-sinkhole features that were extracted. Finally, submodel six extracts the LiDAR derived DEM from the original file by the boundary of the identified sinkhole layer. Therefore, all geometric characteristics can be utilized for analysis. From there, two test locations were used to determine the basis for the model. The model was then applied to nine counties in Iowa. In total, the AIMSINK model identified 47,445 sinkholes in that area.

The AIMSINK model makes use of several ArcGIS tools to calculate these sinkholes. This process is automated, giving it a greater advantage in terms of reducing

time and human error compared to the manual methods that have been utilized in the past. This AIMSINK has several advantages. First, it will save a significant amount of time: the entire study area was completed in 44 hours plus or minus a few hours using a six-core processing computer. Even if it wasn't done on this type of computer, the processing time to complete this would be significantly less compared to heads-up digitizing. Secondly, it minimized human error; therefore, areas that may not have been accounted for will not be missed. Third, sinkhole boundaries have been determined and if needed they can be adjusted through heads-up digitizing. From this it is evident that this model has aided in high-resolution detection and identification of sinkhole boundaries and made it possible to automatically detect them over a large area.

Sinkhole Characteristics and Distribution

Analysis of sinkhole characteristics was then performed. The examined characteristics included geometric sinkhole variables: area, perimeter, width, length, ratio, and depth. The other locational variables consisted of distance to rivers, relative slope, and geology. However, geology was used less frequently in the analysis due to the sinkholes only falling into three geologic units. This was due to a significant statistical problem that arises when trying to incorporate categorical data.

Nearest neighbor clustering analysis and Ripley's K function both identified high amounts of clustering of sinkholes throughout the study region. Therefore, further clustering analysis could be applied.

Correlation analysis illustrated that all planimetric features (shape area, width, length, and ratio) were positively correlated with one another. These correlations were the only strong ones seen; however, there are some less significant but interesting results. As sinkhole surface area increases, depth tends to decrease. Larger planimetric features develop further away from streams, and on flatter slopes. This implies that larger sinkholes tend to develop on higher, flatter interflow areas rather than in valleys near streams. This pattern might relate to age of sinkholes when those developed on drainage divides are likely older and more developed. Sinkholes with longer major axis (ratio increase), tend to be shallower relative to the overall dataset. Sinkholes also tend to be more elongated closer to rivers as slope to a first order stream may cause it to occur. Elongated sinkholes are found on flatter surfaces as well as they merge together forming uvalas. Depth of a sinkhole increases the further away it is from rivers. This pattern is possibly related to lower water tables further from streams, which concentrates sinkhole development in a downward direction rather than lateral growth.

Principal Component Analysis (PCA) identified three main component groups. The 1st component group consisted of a positive output of perimeter, area, width, and length. The 2nd Component group was comprised of a positive output with: ratio (negative correlation), depth, and river distance. The 3rd Component group contained just slope. The results matched well with the patterns elucidated by the correlations.

The K-means cluster method identified five distinct clusters of sinkholes. These clusters are (1) small round and shallow sinkholes, (2) large and shallow, (3) medium deep, (4) small round and deep, and (5) large/medium sinkholes with shallow depth.

Point pattern analysis revealed clustering of sinkholes throughout the study area. LISA and Hotspot analyses identified seven regions. Spatial patterns observed in these regions vary depending on which geometric sinkhole variables or locational variables are considered. However, there are broad similarities between the behaviors of planform variables that differ from sinkhole depth. These LISA and Hotspot clusters correlate well with the PCA illustrating that there is some distinction between the groups. The groups identified (Figure 17) also correlate with geology, which may play a role in the locational development of these geomorphic features. One can speculate that the Galena Group and Platteville formation has a lower water table, as most of the shale creating the aquitard is located at the bottom of the formations, causing the sinkholes to develop at greater depths. It also displays a relatively high joint system as it was identified by geologists mining for lead and zinc, this could be a key factor to depth. There may also be localized regions within these formations that cause certain sinkhole variables to develop more prevalently. However more analysis needs to be performed in order to understand these geologic and geomorphic dynamics these sinkholes display.

Limitations

Methodological Limitations

The methodology and analysis presented in this thesis have a number of limitations primarily related to the data and technical imperfections. First, the AIMSINK process can be applied to each area on a tile by tile basis, utilizing nine tiles (sliding window effect) to check for sinkholes along the edge. However, this approach significantly lengthens data processing time and requires more computing power (and

therefore it was not implemented in this study). The use of smaller tiles will also permit utilizing elevation to provide a more elaborate elevation filter for sinkhole features. The model currently uses Strahler's stream order method to try to eliminate lower elevations. This is because the majority of sinkholes are found on higher elevations, however, due to the low resolution of the Strahler method, this application is not the best suited for removing low lying areas. Nonetheless, this helps to better identify where the sinkholes are located.

The existing Ratio tool developed to determine the ratio of the long and short axis of geometric objects does not accurately represent the overall shape. Some of the features present a curved or thin curved shape erroneously identified as circular feature in some cases. A solution for this problem is creating a circularity tool that actually focuses specifically on circularity.

Determining sinkhole size is another issue to consider. Some sinkholes expand combining into a large valley making it a huge uvula. Therefore, AIMSINK should be able to distinguish between sinkholes and large karst valleys. Currently AIMSINK sets the range for sinkholes between 12 m² and 12,000 m². However, this may vary depending on the location of where this model is being utilized.

Data Errors

A few data problems were identified while working with LiDAR-based elevation data. Since LiDAR has difficulties identifying sinkholes filled with water, it is impossible to account for them in the model. Another problem is a misalignment of road features with the LiDAR data. Another difficulty is larger areas which can be erroneously

identified as sinkholes due to ditches appearing near roads and giving the impression of large elongated sinkholes. Land cover classification may also be an issue with 15 m resolution. As higher-resolution land cover data is implemented in the future, this could be used to determine the sinkhole locations with more accuracy.

Future Work

Future work in this research project could consist of the following. First of all, revising the AIMSINK model and implementing several additional variables and tools, specifically a new circularity tool and local elevation, would create a more accurate representation of the sinkhole layer. Secondly, hypsometric intervals could be calculated to identify overall shape characteristics of sinkholes and if there is any correlation between sinkhole shapes. Thirdly, isolated statistical and spatial analyses on each of the geologic units individually would allow a richer understanding of the role bedrock plays in sinkhole distribution. Fourth, understanding the geologic and geomorphic dynamics of the entire region may help to identify the distribution of these sinkholes more clearly. For example, it is clear that some of these sinkholes follow a linear pattern of a river based on local scale observation. However, this is technically difficult to identify, but something that will be obtainable in the near future.

REFERENCES

- Anderson, W.I. (1983). *Geology of Iowa Over Two Billion Years of Change*. Ames: Iowa State University Press.
- Anderson, W.I. (1998). *Iowa's Geological Past Three Billion Years of Earth History*. Iowa City: University of Iowa Press.
- Anselin, Luc.(1995)."Local Indicators of Spatial Association—LISA," *Geographical Analysis*, 27(2), 93–115.
- Boots, B. N., & Getis, A. (1988). *Point Pattern Analysis*. Newbury Park, CA: Sage Publications.
- Boyer, D. G., & Alloush, G. A. (2001, January 01). Spatial Distribution of Nitrogen On Grazed Karst Landscapes. *The Scientific World Journal*, 1, 809-13.
- Chang, K.-T. (2008). *Introduction to Geographic Information Systems*. Boston, MA: McGraw-Hill.
- Chen, Y., Su, W., Li, J., & Sun, Z. (2009, April 01). Hierarchical Object Oriented Classification Using Very High Resolution Imagery and LIDAR Data Over Urban Areas. *Advances in Space Research*, 43 (7), 1101-1110.
- Denizman, C., (2003). Morphometric and Spatial Distribution Parameters of Karstic Depressions, Lower Suwannee River Basin, Florida. *Journal of Cave and Karst Studies*, 65 (1), 29-35.
- Ebdon, D. (1985). *Statistics in Geography*. Oxford, UK: Oxfordshire: B. Blackwell.
- Field, A. P. (2005). *Discovering Statistics Using SPSS: (and sex, drugs and rock 'n' roll)*. London, UK: Sage Publications.
- Filin, S., Avni, Y., Marco, S., & Baruch, A. (2006). Land Degradation Monitoring Using Airborne Laser Scanning. *Remote Sensing Applications for a Sustainable Future*, 36, (8).
- Ford, D. C., & Williams, P. W. (1989). *Karst Geomorphology and Hydrology*. London, UK: U. Hyman.
- Ford, D. C., & Williams, P. W. (2007). *Karst Hydrogeology and Geomorphology*. Chichester, UK: John Wiley.

- Frye, C. (2008, August 12) Minimum Bounding Rectangle (MBR) Analysis tools. Retrieved November 10, 2012, from ESRI website <http://arcscripts.esri.com/details.asp?dbid=15502>
- Galve, J. P., Gutierrez, F., Lucha, P., Bonachea, J., Remondo, J., Cendrero, A., ... Sanchez, J. A. (2009, January 01). Sinkholes in The Salt-Bearing Evaporite Karst of The Ebro River Valley Upstream of Zaragoza City (NE Spain): Geomorphological Mapping and Analysis as a Basis For Risk Management. *Geomorphology Amsterdam*, 108, 145-158.
- Galve, J. P., Gutierrez, F., Lucha, P., Remondo, J., Bonachea, J., & Cendrero, A. (2009, October 15). Evaluating and Comparing Methods of Sinkhole Susceptibility Mapping in The Ebro Valley Evaporite Karst (NE Spain). *Geomorphology*, 111, 160-172.
- Gao, Y., & Alexander, E. (2008, January 01). Sinkhole Hazard Assessment in Minnesota Using a Decision Tree Model. *Environmental Geology*, 54 (5), 945-956.
- Gao, Y., Alexander, E. C., & Barnes, R. J. (2005, January 01). Karst Database Implementation in Minnesota: Analysis of Sinkhole Distribution. *Environmental Geology Berlin*, 47 (8), 1083-1098.
- Gao, Y., Alexander, E. C., & Tipping, R. G. (2005, January 01). Karst Database Development In Minnesota: Design And Data Assembly. *Environmental Geology Berlin*, 47 (8), 1072-1082.
- GeoTree Center (n.d.). Retrieved August 20, 2012, GeoInformatics Training, Research, Education, and Extension Center (<http://www.geotree.uni.edu/extensions/iowa-lidar-mapping-project/>).
- Getis, A., & Ord, J. K. (1992). The Analysis of Spatial Association By Use of Distance Statistics. *Geographical Analysis*, 24 (3).
- Glennon, A. (2010, February 01). Research Article: Creating and Validating Object-Oriented Geographic Data Models: Modeling Flow within GIS. *Transactions in GIS*, 14 (1), 23-42.
- Groves, J. R., Walters, J. C., Day, J., Hubsher, R., & SEPM Fall Field Conference. (2008). *Carbonate platform facies and faunas of the Middle and Upper Devonian Cedar Valley Group and Lime Creek Formation, Northern Iowa*. Iowa City: Iowa Dept. of Natural Resources.

- Guerrero, J., Gutierrez, F., Bonachea, J., & Lucha, P. (2008, November 12). A Sinkhole Susceptibility Zonation Based on Paleokarst Analysis Along a Stretch of The Madrid–Barcelona High-Speed Railway Built Over Gypsum - and Salt-Bearing Evaporites (NE Spain). *Engineering Geology*, 102, 62-73.
- Gutierrez, F., Cooper, A., & Johnson, K. (2008, January 01). Identification, Prediction, and Mitigation of Sinkhole Hazards in Evaporite Karst Areas. *Environmental Geology*, 53 (5), 1007-1022.
- Hallberg G.R., & Hoyer B.E. (1982). *Sinkholes, Hydrogeology, and Groundwater Quality in Northeast Iowa*. Iowa Department of Natural Resources, Geological Survey Bureau. 82-3, 120.
- Harmon, R. S., Wicks, C. M., Ford, D., & White, W. B. (2006). *Perspectives on Karst Geomorphology, Hydrology, and Geochemistry: A Tribute Volume to Derek C. Ford and William B. White*. Boulder, CO: Geological Society of America.
- Herak, M., & Stringfield, V. (1972). *Karst, Important Karst Regions of The Northern Hemisphere*. Amsterdam, Netherlands: Elsevier Pub. Co.
- Huber, G. (1989). *Sinkholes: Landowner Perceptions of a Unique Source of Groundwater Contamination*. Des Moines, IA: Iowa Natural Heritage Foundation.
- Hyland, S., Kennedy, L., Younos, T., & Parson, S. (2005). *Analysis of Sinkhole Susceptibility and Karst Distribution in The Northern Shenandoah Valley, Virginia: Implications For Low Impact Development (LID) Site Suitability Models*. Blacksburg: University Libraries, Virginia Polytechnic Institute and State University.
- Iowa Department of Natural Resources (2012). Retrieved August 20, 2012, Iowa Department of Natural Resources (ftp://ftp.igsb.uiowa.edu/gis_library/IA_state/geologic/Karst/sinkhole_polys.html).
- Iowa Department of Natural Resources (2013). Retrieved August 20, 2012, Iowa Department of Natural Resources (ftp://ftp.igsb.uiowa.edu/gis_library/IA_state/geologic/Karst/sinkhole_points.html).
- Iowa Department of Natural Resources-Geological Survey Bureau (2000). Retrieved August 20, 2012, Iowa Department of Natural Resources (ftp://ftp.igsb.uiowa.edu/gis_library/IA_state/Hydrologic/Surface_Waters/Stream_order.html).

- Iowa Department of Natural Resources-Geological Survey Bureau (2008). Retrieved August 20, 2012, Iowa Department of Natural Resources (ftp://ftp.igsb.uiowa.edu/gis_library/IA_state/Land_Description/LC_Persistence_1985_2002/persist_85_02.html).
- Iowa Department of Transportation (2007). Retrieved August 20, 2012, Iowa Department of Natural Resources(ftp://ftp.igsb.uiowa.edu/gis_library/IA_state/Infrastructure/Transportation/Iowa_Roads_2006.html).
- Iowa Lidar Consortium. (n.d.). Retrieved August 20, 2012, Iowa Department of Natural Resources (ftp://ftp.igsb.uiowa.edu/gis_library/Projects/Iowa_LiDAR/Block_data/Lidar_LAS_ASCII.html).
- Ivits, E. & Koch, B. (2002, October). *Landscape Connectivity Studies on Segmentation Based Classification and Manual Interpretation of Remote Sensing Data*. eCognition User Meeting, München, Germany.
- Jennings, J. N., (1985). *Karst Geomorphology*. Oxford, UK: B. Blackwell.
- Kimerling, A. J., Buckley, A. R., Muehrcke, P. C., & Muehrcke, J. O., (2012). *Map Use: Reading, Analysis, Interpretation*. Redlands, CA: Esri Press Academic.
- Kruse, S., Grasmueck, M., Weiss, M., & Viggiano, D. (2006, August 28). Sinkhole Structure Imaging in Covered Karst Terrain. *Geophysical Research Letters*, 33 (16).
- Lamelas, M., Marinoni, O., Hoppe, A., & Riva, J. (2008, January 01). Doline Probability Map Using Logistic Regression and GIS Technology in The Central Ebro Basin (Spain). *Environmental Geology*, 54 (5), 963-977.
- LiDAR Image. (n.d.). Retrieved February 20, 2013, from Forest Service University of Washington (http://forsys.cfr.washington.edu/JFSP06/lidar_technology.htm).
- Montane, Juana Maria. (2001). Geophysical Analysis of a Central Florida Karst Terrain using Light Detection and Ranging (LIDAR) and Ground Penetrating Radar (GPR) Derived Surfaces. *Digital Commons. Miami,FL*: Florida International University.
- Ord, J. K., & Getis, A. (1995). Local Spatial Autocorrelation Statistics: Distributional Issues and an Application. *Geographical Analysis*. 27(4).
- Palmquist, R., (1977) *Distribution and Density of Dolines in Areas of Mantled Karst In Dilamarter, R. R., Csallany, S. C., International Symposium on Hydrologic Problems in Karst Regions*, Bowling Green: Western Kentucky University.

- Parise, M., Waele, J., & Gutierrez, F. (2009, January 01). Current Perspectives on The Environmental Impacts and Hazards in Karst. *Environmental Geology*, 58 (2), 235-237.
- Pease, P., Gomez, B., & Schmidt, V., (1994) Magnetostratigraphy of Cave Sediments, Wyandotte Ridge, Crawford County, Indiana: Towards a Regional Correlation. *Geomorphology*, 11, 75-81.
- Podobnikar, T., Scho"ner, M., Jansa, J., & Pfeifer, N. (2008, January 01). Spatial Analysis of Anthropogenic Impact on Karst Geomorphology (Slovenia). *Environmental Geology*, 2, 257-268.
- Prior, J. C. (1991). *Landforms of Iowa*. Iowa City: University of Iowa Press for the Iowa Dept. of Natural Resources.
- Prior, J. C., Grant, S. C., & Geological Society of Iowa. (1975). *Karst Topography Along The Silurian Escarpment in Southern Clayton County, Iowa*. Iowa City, IA: Geological Society of Iowa.
- Ritchie, J. C. (1995, January 01). Airborne Laser Altimeter Measurements of Landscape Topography. *Remote Sensing of Environment*, 53 (2), 91.
- Ritter, D. F. (1978). *Process geomorphology*. Dubuque, IA: W.C. Brown Co.
- Seale, L., Florea, L., Vacher, H., & Brinkmann, R. (2008, January 01). Using ALSM to Map Sinkholes in The Urbanized Covered Karst of Pinellas County, Florida--1, Methodological Considerations. *Environmental Geology*, 54 (5), 995-1005.
- Shofner, J., Mills, H., & Duke, J. (2001, April) A Simple Map Index of Karstification and Its Relationship to Sinkhole and Cave Distribution in Tennessee. *Journal of Cave and Karst Studies*, 63 (2), 67-75.
- Summerfield, M. A. (1997). *Global geomorphology: An Introduction to The Study of Landforms*. Harlow, UK: Longman.
- Sweeting, M. M. (1973). *Karst Landforms*. New York, NY: Columbia University Press.
- Sweeting, M. M. (1981). *Karst Geomorphology*. Stroudsburg, PA: Hutchinson Ross.
- Tarboton, D. G., Bras, R. L. & Rodriguez-Iturbe, I. (1991). On the Extraction of Channel Networks from Digital Elevation Data. *Hydrological Processes*, 5, 81-100.

- U.S. Department of Commerce, U.S. Census Bureau, Geography Division (2010). Retrieved August 20, 2012, Iowa Department of Natural Resources (ftp://ftp.igsb.uiowa.edu/gis_library/IA_state/Admin_Political_Boundary/Incorporated_cities_2010.html).
- Vacher, H. L., Seale, L. D., Florea, L. J., & Brinkmann, R. (2008, January 01). Using ALSM to Map Sinkholes in The Urbanized Covered Karst of Pinellas County, Florida 2. Accuracy Statistics. *Environmental Geology Berlin*, 54 (5), 1007-1015.
- White, W. B. (1988). *Geomorphology and hydrology of karst terrains*. New York, NY: Oxford University Press.
- Whitman, D., Gubbels, T., & Powell, L. (1999, January 01). Spatial Interrelationships between Lake Elevations, Water Tables, and Sinkhole Occurrence in Central Florida: A GIS Approach. *Photogrammetric Engineering and Remote Sensing*, 65 (10), 1169-1178.
- Williams, P. W. (1971, January 01). Illustrating Morphometric Analysis of Karst With Examples From New Guinea. *Zeitschrift für Geomorphologie*, 15
- Wilson, W. L., & Beck, B. F. (1992, November 01). Hydrogeologic Factors Affecting New Sinkhole Development in the Orlando Area, Florida. *Ground Water*, 30 (6), 918-930.
- Witzke, B., Anderson, R., & Pope, J. (2010) Iowa Geological and Water Survey, DNR (ftp://ftp.igsb.uiowa.edu/gis_library/IA_state/Geologic/Bedrock/Bedrock_Geologic_Map.html).
- Wolter, C. F., McKay, R. M., Liu, H., Bounk, M.J., & Libra, R.D. (2011, September) Geologic Mapping for Water Quality Projects in the Upper Iowa River Watershed. *Iowa Geological and Water Survey Technical Information Series*, 54.
- Zhou, W., Beck, B. F., & Adams, A. L. (2003, October 01). Application of Matrix Analysis in Delineating Sinkhole Risk Areas Along Highway (I-70 Near Frederick, Maryland). *Environmental Geology*, 44 (7), 834-842.

APPENDIX

ALMI AND HOTSPOT MAPS

